

# **Stony Brook University**



OFFICIAL COPY

**The official electronic file of this thesis or dissertation is maintained by the University Libraries on behalf of The Graduate School at Stony Brook University.**

**© All Rights Reserved by Author.**

**Synthesis of Inhibitors of the Enoyl Reductase in**

***Mycobacterium tuberculosis.***

A Thesis Presented

by

Christopher William am Ende

to

The Graduate School

in Partial Fulfillment of the

Requirements

for the Degree of

Master of Science

in

Chemistry

Stony Brook University

May 2008

**Stony Brook University**

The Graduate School

**Christopher William am Ende**

We, the thesis committee for the above candidate  
for the Master of Science degree, hereby recommend  
acceptance of this thesis.

Peter J. Tonge, Thesis Advisor  
Professor, Department of Chemistry

Francis Johnson, Chairman of the Thesis Committee  
Professor, Department of Chemistry

Iwao Ojima, Third Member of the Thesis Committee  
Distinguished Professor, Department of Chemistry

This thesis is accepted by the Graduate School

Lawrence Martin  
Dean of the Graduate School

# Abstract of the Thesis

## **Synthesis of Inhibitors of the Enoyl Reductase in *Mycobacterium tuberculosis*.**

by

Christopher William am Ende

Master of Science

in

Chemistry

Stony Brook University

2008

The emergence of multi-drug resistant (MDR) and extensively-drug resistant (XDR) strains of *Mycobacterium tuberculosis* (MTB) has shown that there is an urgent need for the development of novel chemotherapeutics. Previous work has identified a series of alkyl diaryl ethers as effective inhibitors of the enoyl reductase, InhA in MTB, with the most potent compound having a  $K_i'$  of only 1 nM and MIC<sub>99</sub> of 2-3 µg/mL. However, despite promising *in vitro* activities, the *in vivo* activity is poor which may be due to the low solubility of the compounds and lack of slow-onset inhibition. Therefore in an effort to increase the efficacy of their *in vivo* action, a series of compounds were synthesized. Several compounds were identified with comparable MIC values, but possess improved ClogP values. In addition, a compound was identified which shows picomolar inhibition of InhA and which displays a slow, tight-binding mechanism of inhibition.

# Table of Contents

<b>Abstract</b>	<b>iii</b>
<b>List of Figures</b>	<b>vi</b>
<b>List of Schemes</b>	<b>vii</b>
<b>List of Tables</b>	<b>viii</b>
<b>List of Abbreviations</b>	<b>ix</b>
<b>I. Introduction</b>	<b>1</b>
I. 1. Background	1
I. 2. Discovery Process	5
I. 3. Design of Alkyl Diaryl Ethers	7
I. 4. Results and Discussion	8
<b>II. Improving ‘Drug-like’ Properties</b>	<b>13</b>
II. 1. Bioavailability, Lipinski parameters and PSA Background	13
II. 2. Strategies	15
II. 3. Chemistry	15
II. 4. Results and Discussion	18
II. 5. Conclusions	22
<b>III. Slow, Tight-Binding Inhibition</b>	<b>23</b>
III. 1. Background	23
III. 2. The ability enoyl reductases to display slow-onset inhibition	24
II. 2. 1. <i>Francisella tularensis</i> Activity.	25
III. 3. Designing Slow-Onset Inhibition	26

III. 4. Chemistry	27
III. 5. Results and Discussion	27
III. 6. Conclusion	31
<b>IV. Experimental</b>	<b>33</b>
IV. 1. General Procedures for Compound Synthesis	33
IV. 2. Compound Characterization	36
IV. 3. Kinetics Experiments	56
IV. 4. Antibacterial Activity	56
IV. 5. LogP Determination	57
<b>References</b>	<b>59</b>

## List of Figures

Figures	Page
Figure 1. The fatty acid biosynthesis (FASII) pathway in <i>M. tuberculosis</i> .	3
Figure 2. Structures of several inhibitors of the FASII pathway.	4
Figure 3. Crystal structure of triclosan in complex with FabI showing the important hydrogen bonding network between triclosan, the conserved Tyr156 and the NAD <sup>+</sup> cofactor.	7
Figure 4. Overlay of the crystal structure of triclosan bound to InhA and the structure of the C16- <i>N</i> -acetylcysteamine substrate bound. In the C16-NAC/InhA complex, the loop is ordered whereas in the <b>TCN</b> bound structure the loop is disordered.	8
Figure 5. Structures of InhA in complexes with (a) <b>5PP</b> , (b) <b>8PP</b> and (c) <b>INH</b> . The loop termini are shown in red for the <b>5PP</b> and <b>8PP</b> structures. The <b>INH</b> crystal structure displays the ordered active site loop in red.	11
Figure 6. Overlay of crystal structures of <b>a)</b> triclosan bound to FabI and <b>5PP</b> bound to InhA. <b>b)</b> <b>5PP</b> bound to InhA and compound <b>71</b> bound to InhA. Note the similarities in orientation of <b>71</b> to that of <b>TCN</b> .	30
Figure 7. Crystal structures of <b>a)</b> compound <b>71</b> bound to InhA with the ordered loop shown in red. <b>b)</b> Overlay of <b>71</b> with <b>5PP</b> , note the presence of the loop in the <b>71</b> structure. <b>c)</b> A rear view of the <b>71</b> structure showing the solvent accessible aperture that is formed upon loop ordering. <b>d)</b> A rear view of the <b>5PP</b> crystal structure showing the absence of the solvent accessible hole.	32

## List of Schemes

Schemes	Page
Scheme 1. Formation of the INH-NAD(H) adduct.	2
Scheme 2. Synthesis of alkyl diaryl ethers <b>2PP-14PP</b> .	9
Scheme 3. Synthesis of bioisosteric heterocyclic hexyl diaryl ethers <b>22-27</b> .	16
Scheme 4. Synthesis of nitro, amino and amide B-ring substituted hexyl diaryl ethers, <b>34-36</b> , <b>40-42</b> and <b>52-60</b> .	17
Scheme 5. Synthesis of <i>N</i> -methyl piperazine substituted hexyl diaryl ethers, <b>67</b> and <b>68</b> .	18
Scheme 6. Mechanism of inhibition of a) current alkyl diaryl ether inhibitors <b>2PP-14PP</b> . b) of a slow-onset inhibitor such as compound <b>71</b> . Note: $K_i$ is identical to $K_1$ in this scenario. In addition, $K_i^*$ represents both the fast and slow binding steps.	23
Scheme 7. Synthesis of the methyl substituted hexyl diaryl ether, <b>71</b> .	27



## List of Tables

Tables	Page
Table 1. Summary of structure-activity data for triclosan and several analogues toward FabI.	6
Table 2. Alkyl diaryl ether, triclosan and isoniazid enzyme inhibition and MIC <sub>99</sub> data.	10
Table 3. 6PP and heterocyclic B-ring enzyme inhibition, MIC <sub>90</sub> , logP and PSA data.	20
Table 4. 6PP and B-ring substituted enzyme inhibition, MIC <sub>90</sub> , logP and tPSA data.	21
Table 5. Examples of current or previously marketed drugs with slow-onset inhibition.	25
Table 6. <b>6PP</b> , <b>71</b> and <b>INH</b> 's K <sub>i</sub> , K <sub>i</sub> <sup>*</sup> , MIC <sub>99</sub> , ClogP and dissociative t <sub>1/2</sub> data.	29

## List of Abbreviations

°C	degrees centigrade
µg	micrograms
2PP	5-ethyl-2-phenoxyphenol
4PP	5-butyl-2-phenoxyphenol
5PP	5-pentyl-2-phenoxyphenol
6PP	5-hexyl-2-phenoxyphenol
8PP	5-octyl-2-phenoxyphenol
14PP	5-dodecyl-2-phenoxyphenol
Å	angstrom
C16-NAC	hexadecanoyl- <i>N</i> -acetylcysteamine
ClogP	calculated partition coefficient between octanol and water
CoA	coenzyme A
d	doublet
DCE	dichloroethane
DMAc	dimethyl acetamide
ENR	enoyl reductase
ESI-MS	electrospray mass spectrometry
EtOAc	ethyl acetate
EtOH	ethanol
FASII	fatty acid biosynthesis pathway II
GKO	IFN- $\gamma$ gene disrupted mice
H37 <sub>Rv</sub>	strain of MTB
Hex	hexanes
H37 <sub>Rv</sub> pMH29:inha	H37 <sub>Rv</sub> containing an InhA overexpression vector
HTS	high throughput screen
IC <sub>50</sub>	inhibitory concentration at
INH	isoniazid
J	first order coupling constant (NMR)
K	equilibrium constant
k <sub>on</sub>	association constant
k <sub>off</sub>	dissociation constant
logP	partition coefficient between octanol and water
MDR	multidrug resistant
mg	milligram
MIC	minimum inhibitory concentrations
min	minutes
mL	milliliter
MTB	<i>Mycobacterium tuberculosis</i>
MTD	maximum tolerated dose
N.R.	no reaction
N.S.	not soluble
NAD <sup>+</sup>	nicotinamide adenine dinucleotide (oxidized form)

NADH	nicotinamide adenine dinucleotide (reduced form)
NADP <sup>+</sup>	nicotinamide adenine dinucleotide phosphate (oxidized form)
NADPH	nicotinamide adenine dinucleotide phosphate (reduced form)
NHN382	strain of MTB
nM	nanomolar
NMP	n-methyl-2-pyrrolidinone
NMR	nuclear magnetic resonance
pM	picomolar
PSA	polar surface area
q	quartet
r.t.	room temperature
s	singlet
t	triplet
TCN	triclosan
THF	tetrahydrofuran
TN587	strain of MTB
XDR	extensively-drug resistant

## Acknowledgments

I would like to thank Nina Liu and Hua Xu of the Tonge laboratory for the kinetic data, Melissa Boyne and Susan Knudson at Colorado State University for the MIC and animal data and Sylvia Luchner at University of Würzburg for the crystal structures. In addition, I would like to thank Todd J. Sullivan for his mentoring during the initial stages of my graduate career and for helping to complete some of the described synthesis.

I would like to extend a huge thanks to Professor Francis Johnson for advising me on many of the synthetic difficulties that I encountered along the way. Also, Dr. James Marecek for his assistance with difficulties and questions regarding the NMR.

Lastly, I would like to thank my advisor Professor Peter Tonge for his excellent advice and encouragement throughout my stay at Stony Brook University. It was truly a memorable experience.

# Chapter I: Introduction

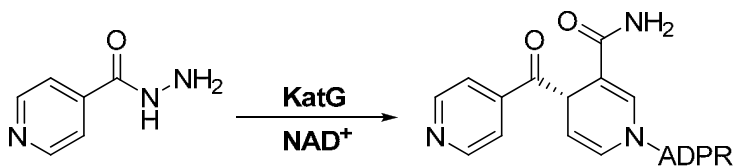
## I. 1. Background

*Mycobacterium tuberculosis* (MTB) has been a prevalent human condition throughout much of the world's history. This can be seen in the evidence of tuberculosis in the skeletal remains of Egyptian mummies as well as in Neolithic man, dating back almost 6000 years ago.<sup>1,2</sup> Hippocrates identified tuberculosis to be one of the most widespread diseases of his times in 460 BC. He even warned his fellow physicians against treating patients who displayed late stage symptoms of the disease, as their impending deaths would surely damage the attending physician's reputation.<sup>3</sup> Furthermore, the disease was also responsible for many deaths throughout the 18<sup>th</sup> and 19<sup>th</sup> centuries. This has resulted in the origin of tuberculosis being blamed on just about every vice or unconventional behavior, including waltzing, until the discovery of the tuberculosis bacilli by Robert Koch in 1882.<sup>3</sup> The discovery of this bacterium opened the doors for the development of new and much improved treatment options.

The history of tuberculosis treatment started with the discovery of streptomycin in 1944 by Selman A. Waksman at the University of California. This represented the first case of a substance capable of reducing the bacterial load. However, this drug was not without side effects and drug-resistant strains emerged within several months.<sup>4</sup> Therefore, it was highly beneficial that many new drugs became available over the next several years. These new drugs

included *p*-aminosalicylic acid (1949), isoniazid (1952), pyrazinamide (1954), cycloserine (1955), ethambutol (1962) and rifampicin (1963).<sup>5-10</sup> However, the emergence of multidrug-resistant (MDR) and extensively-drug resistant (XDR) strains combined with the long and costly treatment demonstrated the urgent need to develop novel chemotherapeutic agents for the treatment of this disease.<sup>11</sup>

The current front-line drug isoniazid (**INH**), targets the synthesis of mycolic acids which are necessary components required in maintaining the integrity of the complex *Mycobacterial* cell wall.<sup>12</sup> Despite the complexity in **INH**'s mechanism of action, there is good evidence that **INH** targets InhA, the enoyl reductase (ENR) in the fatty acid biosynthesis (FASII) pathway (**Figure 1**).<sup>12-15</sup> However, **INH** does not directly target InhA; it first needs to be activated by the catalase-peroxidase enzyme KatG. This activated form of isoniazid then reacts with NAD<sup>+</sup> to form the INH-NAD<sup>+</sup> adduct which is a slow, tight-binding competitive inhibitor of InhA (**Scheme 1**).<sup>17-20</sup> Mutations in KatG account for much of the resistance to **INH**.<sup>21-23</sup> Therefore, it would be desirable to design an inhibitor that can bypass this initial activation step and target InhA directly. Such a compound may display promising activity against many of the drug-resistant strains of *Mycobacterium tuberculosis*.



**Scheme 1.** Formation of the INH-NAD(H) adduct.

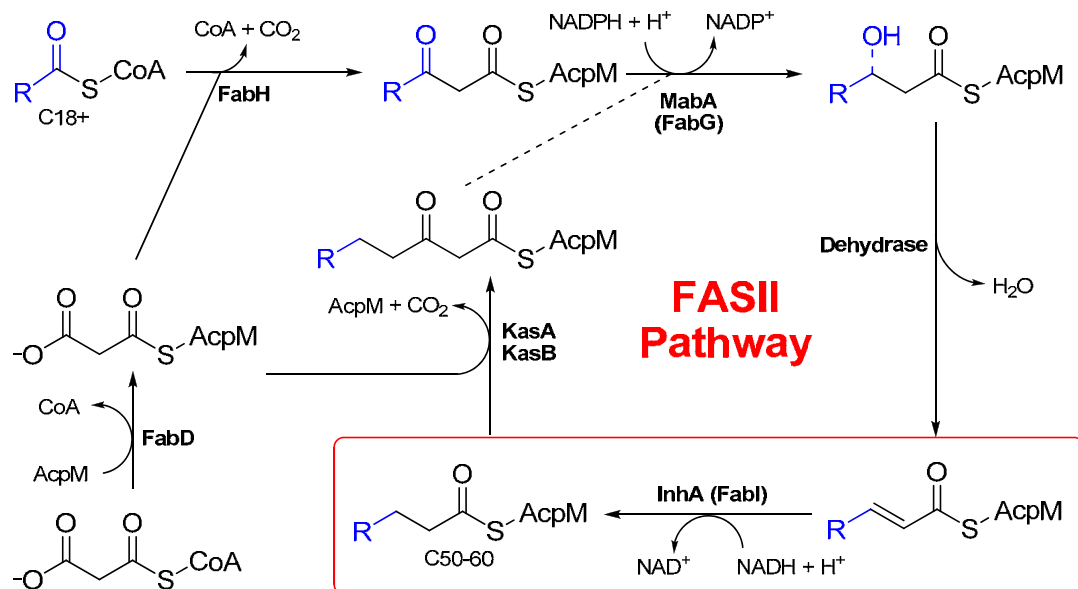


**Figure 1.** The fatty acid biosynthesis (FASII) pathway in *M. tuberculosis*. The FASII pathway in MTB is involved in elongating fatty acids from the FASI cycle. The acyl carrier protein, AcpM, is used to carry the elongating fatty acid through the cycle. AcpM is first condensed with malonyl CoA via FabD, the malonyl CoA:AcpM acyltransferase. The pathway is then initiated another condensation reaction involving the long chain acyl-CoA provided from the FASI pathway with the malonyl-AcpM via FabH, a  $\beta$ -ketoacyl-AcpM synthase III, thereby liberating  $\text{CO}_2$ . Next, the  $\beta$ -ketoacyl-AcpM is reduced by MabA (FabG), a NADPH-dependent 3-ketoacyl-AcpM reductase to the corresponding 3-hydroxy AcpM. This is dehydrated to give the 2-enoyl-AcpM product. The final step involved InhA (FabI), the enoyl-AcpM reductase which reduces the alkene to yield the saturated fatty acid. Successive cycles of elongation are initiated by the condensation of another malonyl-AcpM by either of the  $\beta$ -ketoacyl-AcpM synthases, KasA or KasB with the growing acyl-AcpM product formed from InhA. For each round of this cycle, two carbons are added resulting in a C50-60 fatty acid chain. For a more detailed description of the FASII pathway and its potential as a target for novel chemotherapeutics, refer to Payne *et al.* and references therein.<sup>16</sup>

In addition to the evidence that the INH-NAD<sup>+</sup> adduct targets InhA, there is additional data that supports the notion that the enoyl reductase, InhA (FabI) and other enzymes within the FASII pathway are attractive targets. For example,

there are several known InhA/FabI inhibitors including pyrazole derivatives, indole-5-amides, diazaborines and triclosan which have activity against *M. tuberculosis* and/or other organisms including *Escherichia coli*, *Staphylococcus aureus*, and *Francisella tularensis* (**Figure 2**).<sup>24-29</sup> In addition, other enzymes within the FASII cycle have been shown to be validated drug targets by inhibitors such as thiolactomycin and cerulenin (**Figure 2**).<sup>30-35</sup>

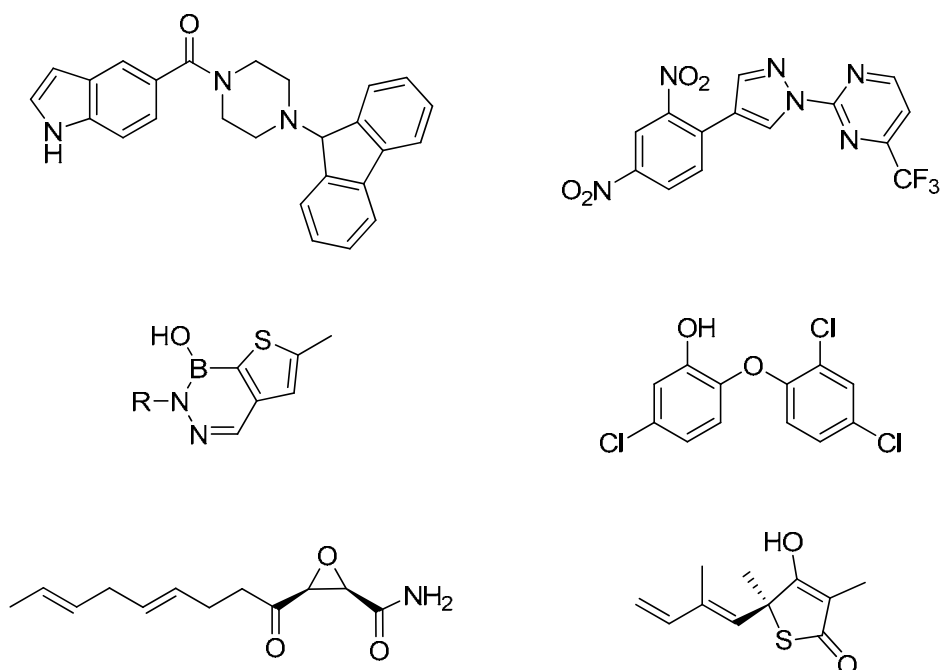


**Figure 2.** Structures of several inhibitors of the FASII pathway.

Furthermore, the fact that the FASII enzymes in MTB differ considerably from the mammalian FAS I pathway which incorporates most of the enzymatic activity into one or two polypeptides, indicates that fatty acid synthesis is an attractive pathway to target.<sup>36,37</sup>

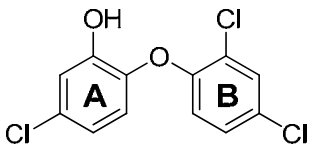
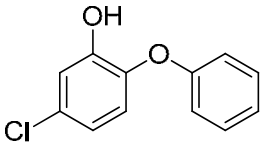
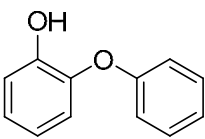


## I. 2. Discovery Process

In order to initiate a design program aimed at developing new inhibitors for a particular enzyme, there are three major approaches that are currently in use. The first incorporates the use of high-throughput screens (HTS), which takes advantage of large screening libraries in order to identify a lead compound. These libraries can range from a few hundred compounds to over 1,000,000.<sup>38-40</sup> This method can also be used *in silico* in order to generate the lead compound.<sup>41-43</sup> The second route which is a growing in popularity as a method for developing new drug candidates, employs the design of transition-state analogues.<sup>44-46</sup> This relies on the idea that a given enzyme has evolved to bind to the transition state of a reaction with the most affinity and therefore the creation of inhibitors that mimic this transient structure should bind tightly within the active site.<sup>45</sup> The third approach is to look into an analogous system and identify the corresponding homologous enzyme where an inhibitor is already known and determine if it can be used as a lead pharmacophore.<sup>47-49</sup> The route that our laboratory took was the latter, with the identification of the lead compound, triclosan (**TCN**, **Figure 2**, **Table 1**).

Triclosan is a common antibacterial found in many consumer products ranging from hand soap to toothpaste. Originally, **TCN** was thought to display a non-specific mode of action. However, recent work has shown that triclosan inhibits FabI, the enoyl reductase in the FASII pathway.<sup>51-54</sup> Specifically it has been shown that, triclosan is a slow, tight-binding uncompetitive inhibitor of the

**Table 1.** Summary of structure-activity data for triclosan and several analogues toward FabI. Refer to Sivaraman *et al.* for a complete analysis.<sup>50</sup>

Compound	Structure	$K_i$ (pM) <sup>a</sup>
TCN		$3.8 \pm 0.2$
1		$0.63 \pm 0.03$
2		$5 \times 10^8$

<sup>a</sup>  $K_i$  is the inhibition constant for uncompetitive inhibition of *E. coli* FabI.

*E. coli* FabI with a  $K_i$  of 7 pM.<sup>50,55</sup> However, Triclosan is a relatively poor inhibitor of InhA with a  $K_i$  of 0.2  $\mu$ M and does not display slow-onset inhibition.<sup>56</sup> Therefore, detailed kinetic and crystallographic as well as structure-activity relationship studies were initially performed on the *E. coli* FabI in order to determine the necessary functionality on the molecule. The results of these studies are reported in Sivaraman *et al.* and summarized in **Figure 3** and **Table 1**.<sup>50,57</sup> The outcome of these experiments shows the considerable importance of the 5'-chlorine on the A-ring as well as the relative insignificance of the B-ring chlorines. These data coupled with a crystal structure of **TCN** bound to FabI, show the significance of the phenol and bridging oxygen because they are involved in a hydrogen-bonding network with a conserved tyrosine residue as well as the NAD<sup>+</sup> cofactor (**Figure 3**).<sup>57</sup>

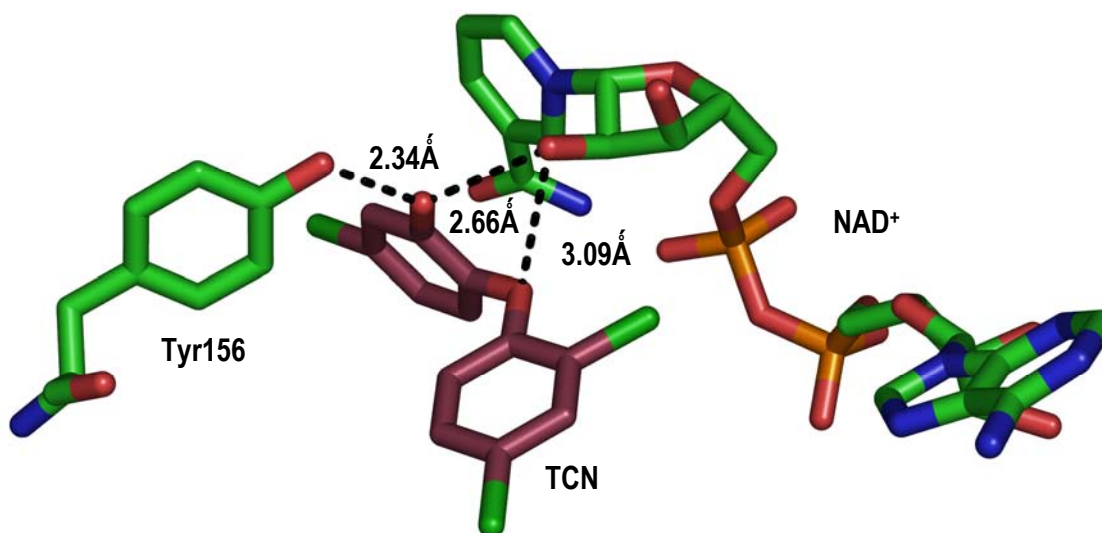


**Figure 3.** Crystal structure of triclosan in complex with FabI showing the important hydrogen bonding network between triclosan, the conserved Tyr156 and the NAD<sup>+</sup> cofactor.

### I. 3. Design of Alkyl Diaryl Ethers

In order to design inhibitors for InhA, analyses of both substrate specificity and structural data were performed. It is known that InhA has a larger substrate-binding loop than FabI and therefore may tolerate larger substituents.<sup>58</sup> Moreover, a crystal structure of triclosan bound to InhA was obtained.<sup>59</sup> This crystal structure overlaid with the crystal structure of a hexadecanoyl-*N*-acetylcysteamine (**C16-NAC**) substrate bound to InhA show the 5'-chlorine is directed into the same hydrophobic pocket in which the alkyl chain of the fatty acid is normally bound (**Figure 4**).<sup>58,59</sup> Consequently, in order to mimic the way the substrate binds within the active site and to take advantage of the larger substrate binding pocket, inhibitors were synthesized with alkyl chains of varying

lengths at the 5-position on the A-ring as shown in **Scheme 2** and the results of which are summarized in **Table 1**.<sup>59</sup>

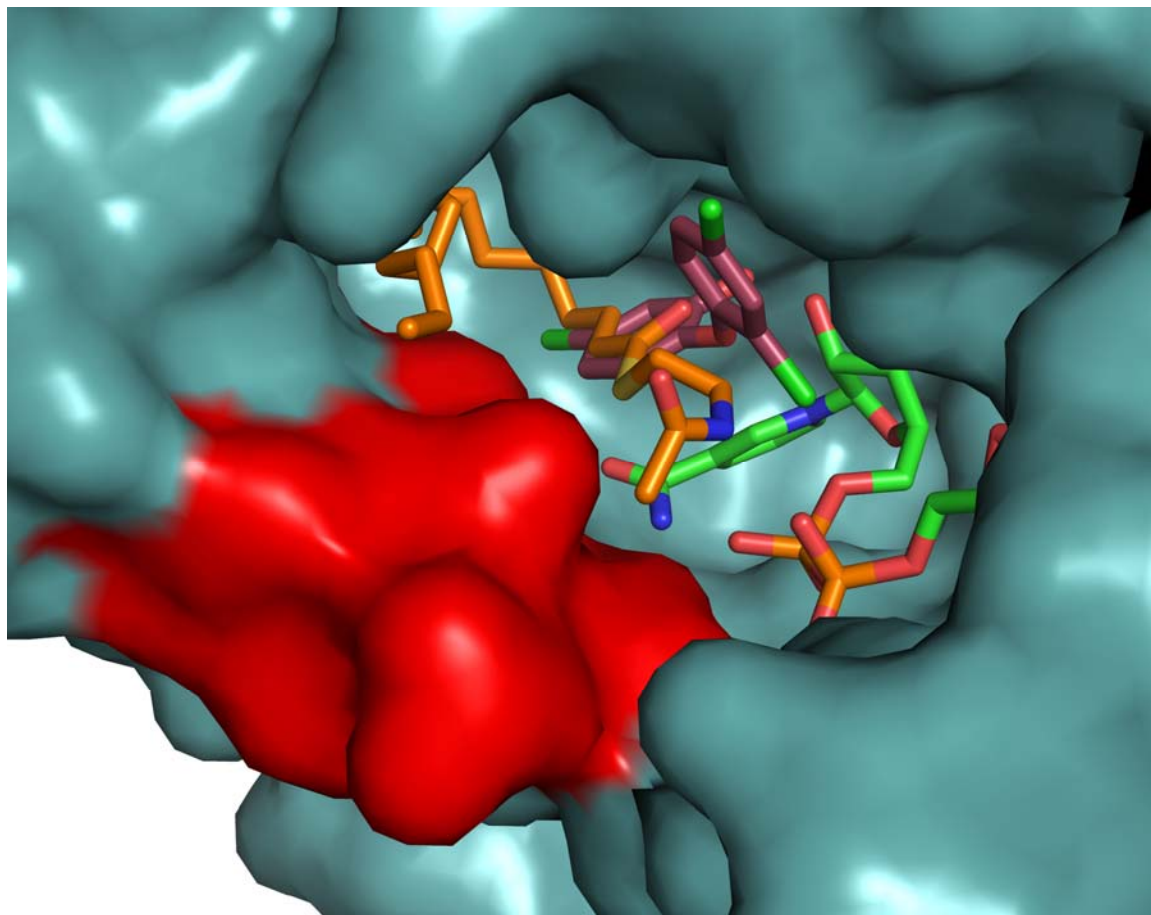
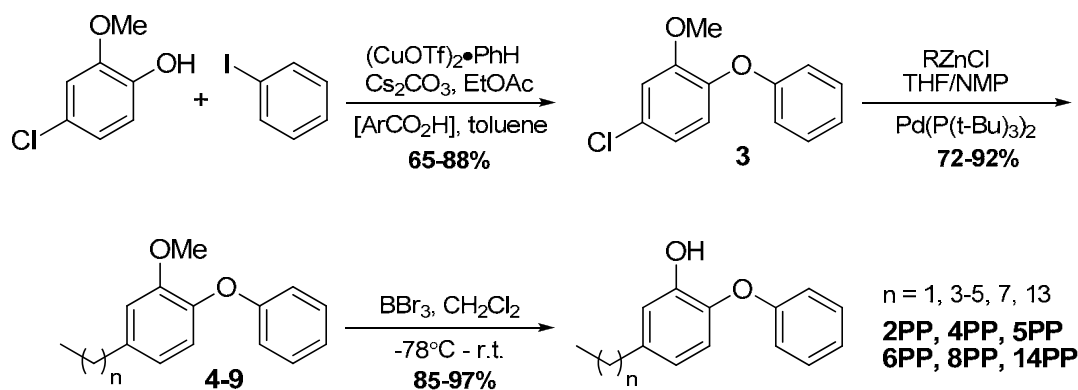


**Figure 4.** Overlay of the crystal structure of triclosan bound to InhA and the structure of the C16-*N*-acetylcysteamine substrate bound. In the C16-NAC/InhA complex, the loop is ordered whereas in the TCN bound structure the loop is disordered.

#### I. 4. Results and Discussion

It is demonstrated in **Table 2** that increasing the length of the alkyl chain has beneficial effects on inhibitor binding. Specifically, the ethyl diaryl ether, **2PP** has an  $IC_{50}$  of 2000 nM whereas increasing the alkyl chain by two carbons to the



**Scheme 2.** Synthesis of alkyl diaryl ethers **2PP-14PP**.

butyl, decreases the  $IC_{50}$  value 25-fold. A further increase of the alkyl chain to 8 carbons decreases the  $IC_{50}$  value another 16-fold and results in a  $K_i$  of  $1.1 \pm 0.2$  for **8PP**. However, when the alkyl chain is increased further to 14 carbons, there is a negative effect on inhibition with **14PP** showing a  $K_i'$  of  $30.3 \pm 4.7$ .<sup>59</sup>

More importantly, the  $MIC_{99}$  values in **Table 2** show that there is activity against several strains of MTB with varying sensitivities to **INH**. It can be seen that these  $MIC_{99}$  values are a significant improvement to those displayed by **TCN** and are approaching the values that the current front-line drug isoniazid exhibits. In addition, the H37<sub>Rv</sub> pMH29:*inhA* strain of MTB contains an *InhA* overexpression vector and therefore, the increased  $MIC_{99}$  value that is observed is consistent with the inhibitors mainly targeting *InhA* within the cell and not other enzymes within the cell.<sup>59</sup> This is also demonstrated by the good correlation between the  $K_i$  and  $MIC$  data.

Fortunately, crystal structures of both the **5PP** and **8PP** inhibitors bound to *InhA* were obtained by our collaborators in the University of Würzburg. It can be seen that these inhibitors bind in a similar manner to triclosan, retaining the

hydrogen-bonding network and placing the alkyl chain into the desired hydrophobic, substrate-binding pocket (**Figure 5a and b**).<sup>59</sup>

**Table 2.** Alkyl diaryl ether, triclosan and isoniazid enzyme inhibition and MIC<sub>99</sub> data.

Compound <sup>a</sup>	IC <sub>50</sub> (nM) <sup>b</sup>	K <sub>i</sub> <sup>c</sup> (nM)	MIC <sub>99</sub> µg/mL (µM) <sup>d</sup>			
			H37 <sub>Rv</sub>	H37 <sub>Rv</sub> pMH29:inhA <sup>e</sup>	TN587	NHN382
TCN	1000 ± 100	220 ± 20	12.5 ± 0 (43.1 ± 0)	33.3 ± 12.9 (115 ± 45)		
2PP	2000 ± 700		3.8 ± 0 (17.5 ± 0)			
4PP	80 ± 15		2.6 ± 0.8 (10.8 ± 3.3)			
5PP	17 ± 5	11.8 ± 4.5	1.0 ± 0 (3.5 ± 0)			
6PP	11 ± 1	9.4 ± 0.5	2.1 ± 0.9 (7.8 ± 3.3)	18.8 ± 6.8 (69 ± 25)	2.0 ± 1.0 (7.4 ± 3.7)	3.1 ± 0 (11.5 ± 0)
8PP	5.0 ± 0.3	1.1 ± 0.2	1.9 ± 0.5 (6.4 ± 1.7)	22.9 ± 5.1 (77 ± 17)	2.0 ± 1.0 (6.7 ± 3.4)	2.6 ± 0.9 (8.7 ± 3.0)
14PP	150 ± 24	30.3 ± 4.7	175 (460)			
INH		0.75 ± 0.08 <sup>f</sup>	0.05 ± 0 (0.37 ± 0)		2.4 ± 1.3 (17.5 ± 9.5)	1.6 ± 0 (11.7 ± 0)

<sup>a</sup>2PP, 4PP, 5PP, 6PP, 8PP and 14PP represent the diaryl ethers containing ethyl, butyl, pentyl, hexyl, octyl, and tetradecyl substituents at the 5 position. <sup>b</sup>IC<sub>50</sub> measurements determined via varying inhibitor concentration at fixed substrate concentration. <sup>c</sup>K<sub>i</sub> is the inhibition constant for uncompetitive inhibition of InhA. <sup>d</sup>MIC<sub>99</sub> is the concentration of inhibitor need to result in complete inhibition of MTB cell growth. H37<sub>Rv</sub> is a drug-sensitive strain of MTB, whereas TN587 and NHN382 are clinical strains of MTB with various sensitivities toward INH. Data on additional strains can be found in Sullivan *et al.*<sup>59</sup> <sup>e</sup>H37<sub>Rv</sub> pMH29:inhA is a strain of MTB containing an overexpression vector for InhA. <sup>f</sup>K<sub>i</sub> for the INH-NAD adduct can be found in Rawat *et al.*<sup>20</sup>

An important point to note from these crystal structures and from the kinetic data, is that these inhibitors do not display the slow-onset inhibition that is seen with

the INH-NAD<sup>+</sup> adduct or with triclosan bound to FabI.<sup>20,55,56</sup> This is evident in the crystal structures by the absence of electron density in the active site loop region

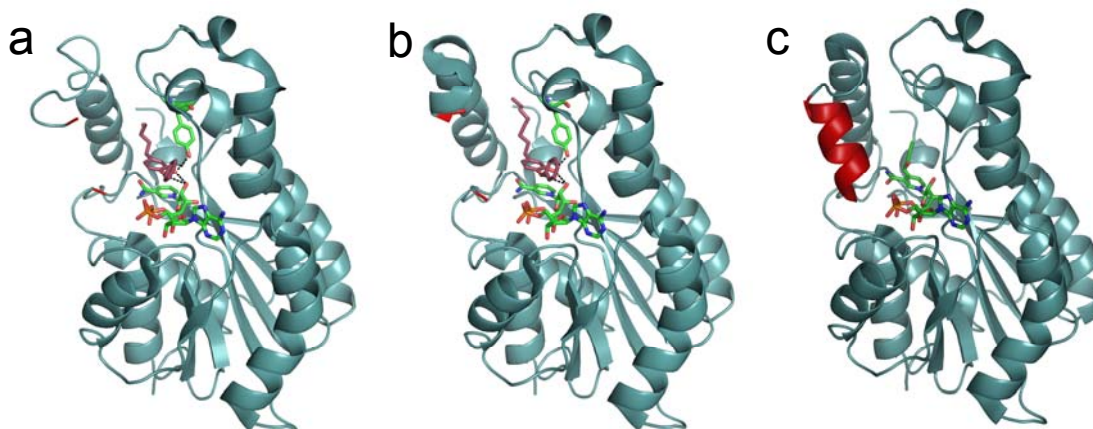


**Figure 5.** Structures of InhA in complexes with (a) **5PP**, (b) **8PP** and (c) **INH**. The loop termini are shown in red for the **5PP** and **8PP** structures. The **INH** crystal structure displays the ordered active site loop in red.

whereas these residues are seen in the **INH** crystal structure (**Figure 5c**).<sup>26,60</sup> Importantly, the structural data provide an important foundation that will aid in the generation of new inhibitors via simple crystal structure analysis and computational methods such as molecular modeling and docking experiments. It is hoped that these methods will lead to an improvement in inhibition as well as invoke active site loop ordering.

The MIC<sub>99</sub> values of both the **6PP** and **8PP** inhibitors were in the acceptable range for testing in a rapid animal model of MTB infection using IFN- $\gamma$  gene disrupted (GKO) mice. These compounds were shown to have a maximum tolerated dose (MTD) of > 500 mg/kg with no adverse side effects observed after 7 days following a single dose of 100, 300, or 500 mg/kg. However, the concentration of these inhibitors in the serum was determined to be ~20  $\mu$ g/mL at

30 minutes after dosing corresponding to a low to medium bioavailability. Consistent with this low value, both **6PP** and **8PP** were unable to reduce the bacterial load within the lungs and spleen.<sup>61</sup> Therefore, the problem of low bioavailability needs to be addressed in this series.



## Chapter II: Improving 'Drug-like' Properties

### II. 1. Bioavailability, Lipinski parameters and PSA Background

Bioavailability of a compound is a major hurdle in the development of new drugs and is often a parameter that disqualifies an inhibitor from further trials regardless of how effective it is *in vitro*. The bioavailability of a drug is described as the fraction of the administered dose that reaches the systemic circulation i.e. bioavailability is a reason for the difference between the dose and exposure.<sup>62-65</sup> Therefore, by definition an intravenous route of administration results in 100% bioavailability. However, there are many reasons that a drug should have oral bioavailability due to a practical stand point for ease of administration.<sup>63,64</sup> Many factors influence the oral bioavailability of a drug including solubility and first-pass metabolism in addition to other factors resulting in compound elimination.<sup>63,65</sup> Furthermore, there are several simple molecular descriptors that have been correlated with oral bioavailability with one assessment outlined by Lipinski *et al.*<sup>66</sup>

Christopher Lipinski at Pfizer Global Research and Development set out to determine factors that influence the 'drug-likeness' of a compound in order to understand which parameters are important in the drug discovery process. Through statistical analysis there were four descriptors that were determined to be common features in orally administered drugs. They showed that an orally bioavailable drug has:

1. Not more than 5 hydrogen bond donors.
2. Not more than 10 hydrogen bond acceptors.
3. A molecular weight less than 500 g/mol.
4. A ClogP under 5.

Due to the common denominator of 5 throughout the rules, they gave it the name 'the rule of five' and termed it a predictor of poor absorption and permeation if a compound did not fall within these parameters.<sup>66</sup> These compounds fail only one of the rules with both **6PP** and **8PP** outside the desired ClogP value of less than 5. Respectively, they have ClogPs of 6.47 and 7.53 (**Table 3**).

Another descriptor that is commonly used in determining whether a compound will have good oral bioavailability is its polar surface area (PSA).<sup>63,67-70</sup> PSA is the sum of the van der Waals surface area from oxygen or nitrogen atoms within a compound as well as the hydrogen atoms attached to them.<sup>71</sup> Therefore, it is obviously directly correlated with a molecule's hydrogen bonding ability. A study performed by GlaxoSmithKline indicates that a PSA less than 140 Å<sup>2</sup> will have a high possibility of good oral bioavailability.<sup>62</sup> Therefore, in an effort to increase the 'drug-like' properties of our compounds, a series of compounds were synthesized in an effort to decrease ClogP while retaining PSA values below the 140 Å<sup>2</sup> maximum value.<sup>70</sup>

## II. 2. Strategies

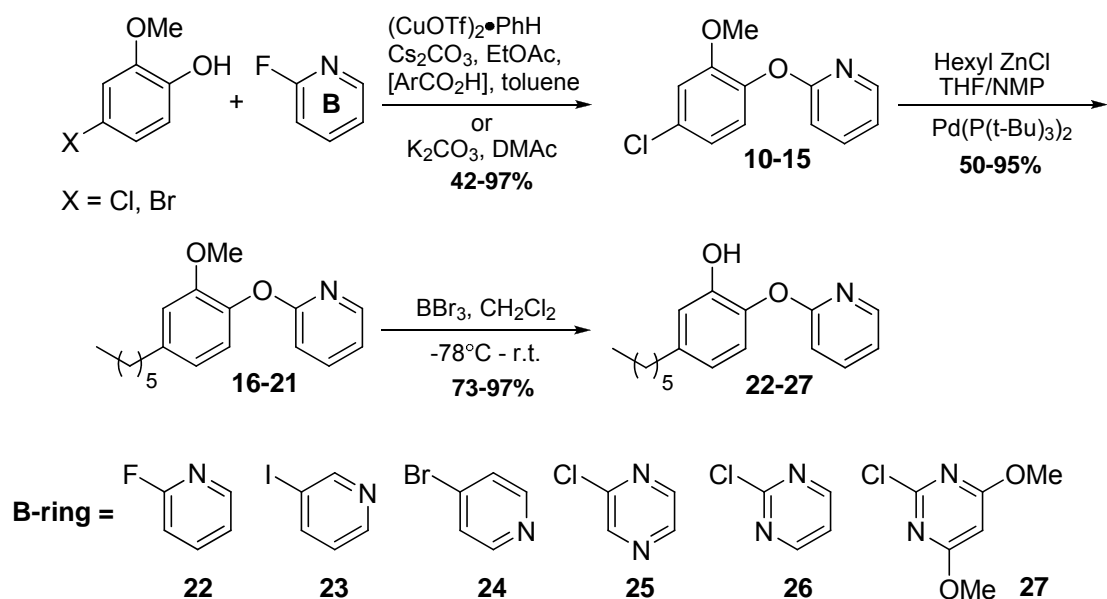
In order to accomplish the goal of decreasing the ClogP values for these compounds, two classes of molecules were synthesized with alterations to the diaryl ether B-ring. In one series of compounds the B-ring was replaced with bioisosteric heterocycles which incorporate nitrogen atoms within the ring in an effort to cause minimal steric perturbation to the overall structure of the molecule (**Scheme 3**). The second series of compounds contains nitro, amino, amide and piperazine functionalities at the *ortho*, *meta* and *para* positions on the B-ring (**Scheme 4 and 5**). This series was synthesized in an effort not only to increase aqueous solubility but also to systematically explore the chemical space around the ring in order to identify positions which could be substituted without diminishing biological activity. A portion of this work can be found in Bioorganic and Medicinal Chemistry Letters with kinetic data performed by Nina Liu and MIC data performed by Susan Knudson at Colorado State University.

## II. 3. Chemistry

The synthesis of the heterocyclic diaryl ether compounds was initiated either by nucleophilic aromatic substitution or Buchwald-Hartwig cross coupling of the appropriate nitrogen heterocycle with 4-bromo or chloro-2-methoxy phenol producing **10-15** (**Scheme 3**).<sup>72,73</sup> This was followed by palladium-catalyzed Negishi coupling of the diaryl ethers with hexyl zinc chloride to give **16-21**. Boron

tribromide cleavage of the methyl ether was subsequently used to generate the respective phenols, **22-27**.<sup>74</sup> Structural characterization of all compounds was performed using <sup>1</sup>H NMR and ESI/MS.

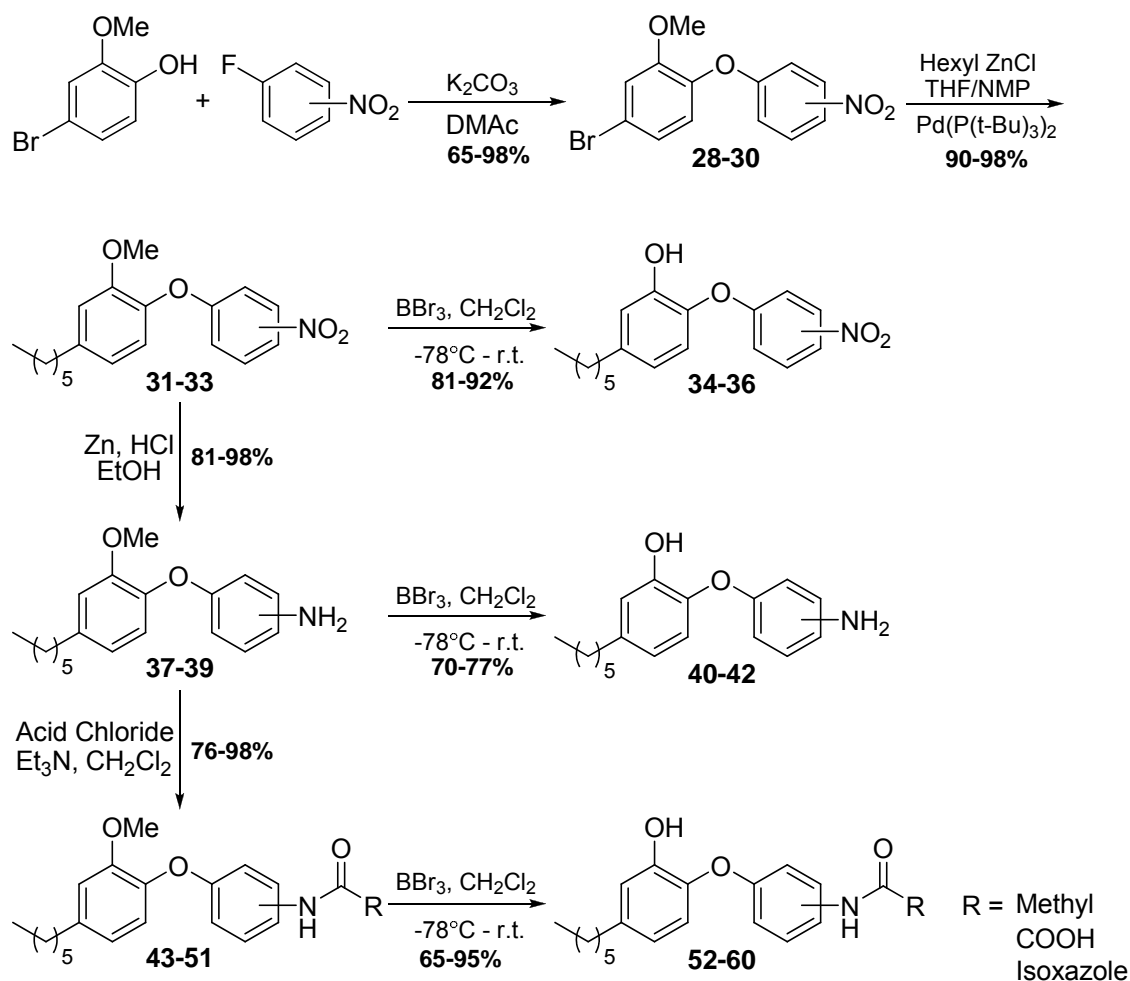
The syntheses of the nitro, amino and amide-substituted compounds were performed using the series of reactions shown in **Scheme 4**. Nucleophilic aromatic substitution reactions with fluoro nitrobenzene were first used to



**Scheme 3.** Synthesis of bioisosteric heterocyclic hexyl diaryl ethers **22-27**.

generate compounds **28-30**.<sup>73</sup> This was followed by Negishi coupling giving **31-33** with boron tribromide cleavage of the methyl ether resulting in phenols **34-36** or zinc-mediated reduction resulting in the anilines **37-39**.<sup>74-76</sup> Cleavage of the methyl ether gave **40-42** whereas acylation of the anilines with acyl chlorides afforded compounds **43-51**.<sup>74,77</sup> Boron tribromide cleavage furnished the final compounds **52-60**.<sup>74</sup>

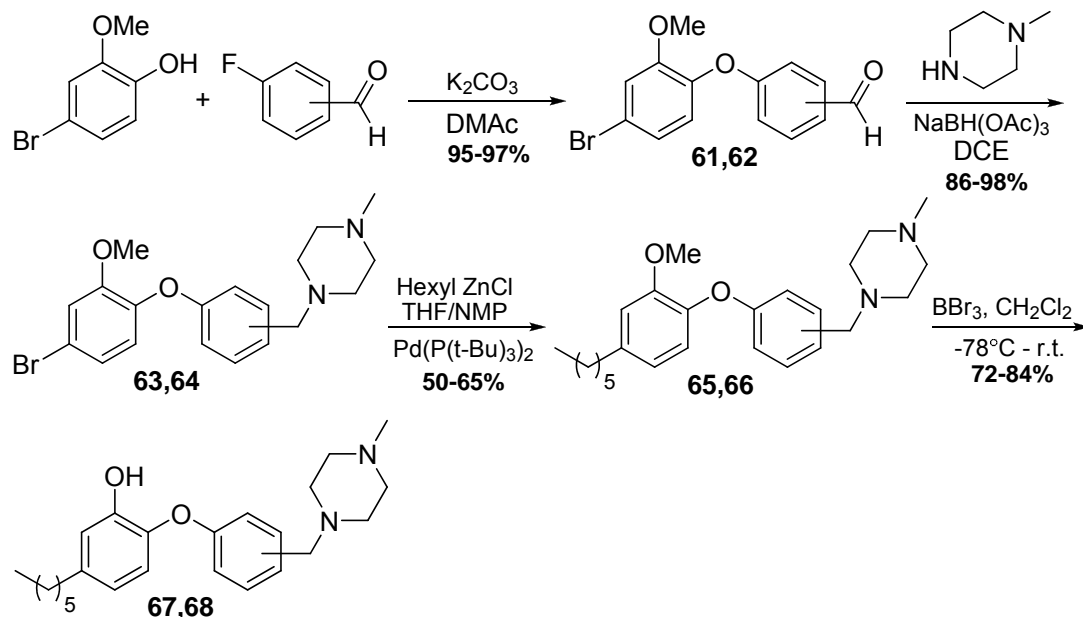
The piperazine derivatives were synthesized in a similar fashion starting with nucleophilic aromatic substitution with the 2 or 4-fluorobenzaldehyde to give **61** and **62** (Scheme 5).<sup>73</sup> Subsequently, reductive amination with methyl piperazine and sodium triacetoxyborohydride produced **63** and **64**,<sup>78</sup> whereas Negishi coupling followed by boron tribromide cleavage gave final compounds **67** and **68**.<sup>74,76</sup>



**Scheme 4.** Synthesis of nitro, amino and amide B-ring substituted hexyl diaryl ethers, **34-36**, **40-42** and **52-60**.

## II. 4. Results and Discussion

The *in vitro* activities of the final products were evaluated using enzyme inhibition and whole cell antibacterial assays as described (**Tables 3 and 4**).<sup>13,36,59</sup> In general, addition of a bulky substituent at either the ortho, meta or para position of the B ring of **6PP** or its substitution by most nitrogen heterocycles resulted in significant reduction in enzyme inhibition and antibacterial activity (**Table 4**). However, the smaller aniline substituent was tolerated at the ortho



**Scheme 5.** Synthesis of *N*-methyl piperazine substituted hexyl diaryl ethers, **67** and **68**.

and para positions as well as the nitro group at the meta position (**Table 4**). The three most active compounds, **23**, **24** and **40**, all have  $MIC_{90}$  values of 3.13  $\mu g/mL$ , which is comparable to **6PP**, and have ClogP values of 4.97 and 5.24,

respectively, compared to 6.47 for the parent compound (**Tables 3 and 4**). In addition it is also worth noting that the pyrazine derivative, **25** has a ClogP value that is more than a 2.5 units lower than **6PP** and only shows only a 3-fold increase in MIC<sub>90</sub> compared to the parent (**Table 3**). In general the MIC values paralleled the IC<sub>50</sub> values for enzyme inhibition. Thus ortho and para amino substituents (**40 and 42**) were well tolerated in addition to the meta nitro substituent (**35**). In these three cases the IC<sub>50</sub> values obtained using 100 nM InhA approached 50% of the enzyme concentration, indicating that these compounds are tight-binding enzyme inhibitors. Additional IC<sub>50</sub> values were determined using 10 and 50 nM InhA in the enzyme assays. Subsequent linear regression of the IC<sub>50</sub> values as a function of enzyme concentration yielded estimates for  $K_i^{app}$  of  $21 \pm 3$  nM (**35**),  $16 \pm 12$  nM (**40**) and  $40 \pm 3$  nM (**42**). Thus, introduction of meta NO<sub>2</sub> (**35**) or ortho NH<sub>2</sub> (**40**) substituents into the B ring of the parent compound **6PP** has only a minor effect on affinity of the inhibitor for the enzyme. In addition, all compounds retained PSA values that were below the maximum value of 140 Å<sup>2</sup>.

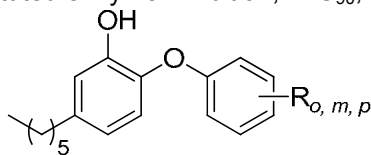
**Table 3.** 6PP and heterocyclic B-ring enzyme inhibition, MIC<sub>90</sub>, logP and PSA data.

Compound	Structure	IC <sub>50</sub> (nM) <sup>a</sup>	MIC <sub>90</sub> μg/mL (μM) <sup>b</sup> H37 <sub>RV</sub>	ClogP <sup>c</sup> (logP) <sup>d</sup>	PSA <sup>c</sup>
6PP		11 ± 1 <sup>e</sup>	2.1 ± 0.9 (7.8 ± 3.3)	6.47 (5.76)	29.46
22		11510 ± 1160	50 (184)	4.97 (5.06)	41.82
23		236 ± 31	3.13 (11.5)	4.97	41.82
24		160.6 ± 15.8	3.13 (11.5)	4.97 (4.93)	41.82
25		653 ± 56	6.25 (22.9)	4.01 (4.46)	54.18
26		8200 ± 980	100 ± 0 (367 ± 0)	4.01 (4.76)	54.18
27		N.S. <sup>f</sup>	N.S. <sup>f</sup>	5.50	72.64

<sup>a</sup>IC<sub>50</sub> measurements determined via varying inhibitor concentration at a fixed substrate concentration of 100nM. <sup>b</sup>MIC<sub>90</sub> is the concentration of inhibitor need to result in complete inhibition of MTB cell growth. H37<sub>RV</sub> is a drug-sensitive strain of MTB. <sup>c</sup>ClogP and tPSA values determined using ChemDraw version 11.0. <sup>d</sup>logP values determined via HPLC methods as described in the experimental by James Childs and Charles Peloquin. <sup>e</sup>IC<sub>50</sub> determined at enzyme concentration of 1nM as described in Sullivan *et al.*<sup>59</sup> <sup>f</sup>Compound was not soluble under assay conditions.



**Table 4.** 6PP and B-ring substituted enzyme inhibition, MIC<sub>90</sub>, logP and tPSA data.



Compound	Structure	IC <sub>50</sub> (nM) <sup>a</sup>	MIC <sub>90</sub> µg/mL		ClogP <sup>c</sup> (logP) <sup>d</sup>	tPSA <sup>c</sup>
			H37 <sub>RV</sub> <sup>b</sup>			
34		<i>o</i> 182.4 ± 20	12.50		6.21 (5.50)	81.27
35		<i>m</i> 48 ± 6	12.50		6.21	81.27
36		<i>p</i> 90 ± 10	25.0 ± 0		6.21 (5.64)	81.27
40		<i>o</i> 61.9 ± 4.5	3.13		5.24 (5.27)	55.48
41		<i>m</i> 1090 ± 90	100 ± 0		5.24	55.48
42		<i>p</i> 55 ± 6	12.50		5.24 (4.93)	55.48
52		<i>o</i> 1550 ± 460	> 200		4.90 (5.28)	58.56
53		<i>m</i> N.S. <sup>e</sup>	N.S. <sup>e</sup>		4.90	58.56
54		<i>p</i> 1310 ± 170	50.0 ± 0		4.90	58.56
55		<i>o</i> 2630 ± 200	100.0		4.24	95.86
56		<i>m</i> 579 ± 36	133.3 ± 57.7		4.24	95.86
57		<i>p</i> 1930 ± 90	> 200		4.24	95.86
58		<i>o</i> 3220 ± 550	> 200		5.76 (5.60)	80.15
59		<i>m</i> 1220 ± 60	> 200		5.76 (5.22)	80.15
60		<i>p</i> 130 ± 34	> 200		5.76 (5.15)	80.15
67		<i>o</i> 1325 ± 256	100		6.66	35.94
68		<i>p</i> 306 ± 46	100		6.66	35.94

<sup>a</sup>IC<sub>50</sub> measurements determined via varying inhibitor concentration at a fixed substrate concentration of 100nM. <sup>b</sup>MIC<sub>90</sub> is the concentration of inhibitor need to result in complete inhibition of MTB cell growth. H37<sub>RV</sub> is a drug-sensitive strain of MTB. <sup>c</sup>ClogP and tPSA values determined using ChemDraw version 11.0. <sup>d</sup>logP values determined via HPLC methods as described in the experimental by James Childs and Charles Peloquin. <sup>e</sup>Compound was not soluble under assay conditions.

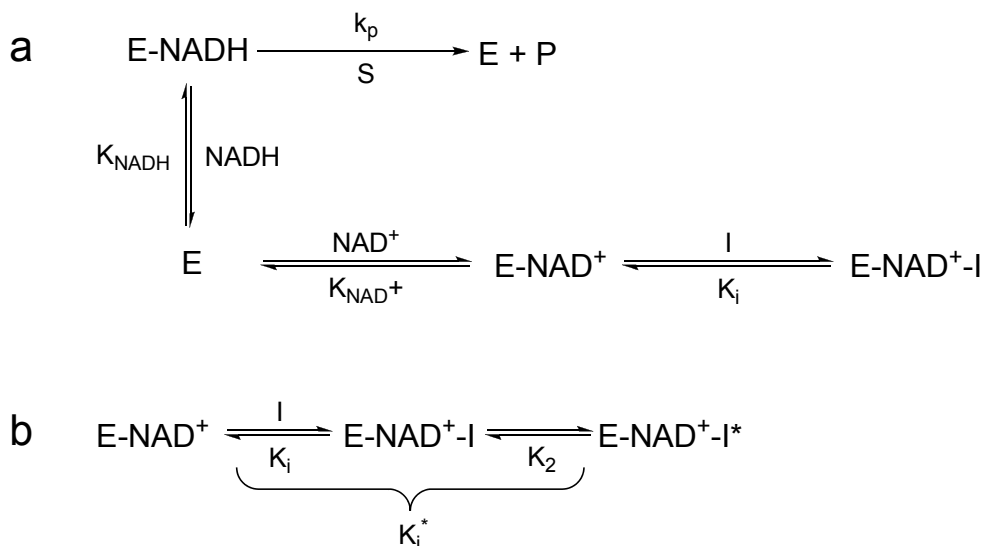
## II. 5. Conclusions

In conclusion, several compounds were synthesized which incorporated either bioisosteric heterocycles in place of the B-ring or substitutions at the *ortho*, *meta* or *para* positions of the B-ring. In general, most of the compounds accomplished the goal of decreasing ClogP values with several compounds showing promising *in vitro* activity. For example, compounds **35** and **40** showed comparable  $K_i^{app}$  to the parent compound **6PP**, whereas **23**, **24** and **40** displayed similar MIC values. Therefore, it has been shown that InhA can tolerate smaller substituents at all positions on the B-ring as well as meta and para pyridines as replacements of the B-ring while retaining activity, decreasing ClogP values and retaining PSA values within acceptable ranges.

### III. Slow, Tight-binding Inhibition

#### III. 1. Background

Enzyme inhibition can be a complex issue due to the numerous ways in which small molecule inhibition can occur. For example, one can observe competitive, uncompetitive or noncompetitive inhibition which can be broken down further to reversible, irreversible and slow-onset.<sup>79</sup> Currently all of our inhibitors display a classical uncompetitive tight-binding mode of inhibition (**Scheme 6a**).<sup>59</sup> However, it is desirable to obtain slow-onset inhibition since this can lead to improved *in vivo* characteristics (**Scheme 6b**).<sup>20,80-82</sup>



**Scheme 6.** Mechanism of inhibition of **a**) current alkyl diaryl ether inhibitors **2PP-14PP**. **b**) of a slow-onset inhibitor such as compound **71**. Note:  $K_i$  is identical to  $K_1$  in this scenario. In addition,  $K_i^*$  represents both the fast and slow binding steps.

An excellent paper by Copeland *et al.* proposes that a more important factor for *in vivo* drug potency is the residence time of the drug on its target and not necessarily its apparent affinity towards that target. Specifically, one can imagine that an increased time of interaction between an inhibitor and its target will lead to a longer effect of drug action as the enzyme is effectively inactivated for a significant period of time. Furthermore, when describing an *in vivo* case, the concentration of inhibitor does not remain constant and therefore, typical *in vitro* measurements of the inhibition constant ( $K_i$ ) are not accurate descriptors of how efficacious an inhibitor will be in an *in vivo* environment. This is because traditional measurements of  $K_i$  are only representative of the first step in the slow-binding inhibition mechanism (**Scheme 6b**). A more important consideration would be the association rate constant ( $k_{on}$ ) and more importantly, the dissociation rate constant ( $k_{off}$ ). The  $k_{off}$  value is directly related to the residence time of the inhibitor on its target and therefore,  $K_i^*$  is a more accurate descriptor of this.<sup>80</sup> Moreover, there are many examples of current or previously marketed drugs that display this slow-onset inhibition as revealed in **Table 5**.<sup>20,83-</sup>

87

### III. 2. The ability of enoyl reductases to display slow-onset inhibition.

In addition to the examples shown in **Table 5**, there is direct evidence that InhA is capable of displaying slow-onset inhibition if the proper compound is found that will allow for it.<sup>20</sup> Specifically, as described in the introduction, the

**Table 5.** Examples of current or previously marketed drugs with slow-onset inhibition

Marketed Name	Inhibitor	Enzyme	Dissociative $t_{1/2}$
Proloprim	Trimethoprim	<i>E. coli</i> dihydrofolate reductase	8 minutes <sup>83</sup>
Capoten	Captopril	Angiotension converting enzyme	30 minutes <sup>84</sup>
Isoniazid	INH-NAD <sup>+</sup>	MTB enoyl reductase	41 minutes <sup>20</sup>
Tamiflu	Oseltamivir	Viral neuroaminidase	47 minutes <sup>85</sup>
Atacand	Candesartan	Human angiotension II type 1 receptor	1-3 hours <sup>86</sup>
Vioxx	Rofecoxib	COX2	9 hours <sup>87</sup>

*E. coli* FabI is inhibited by **TCN** via slow, tight-binding inhibition.<sup>50,55</sup> Crystal structure analysis of this interaction shows that there is a substrate binding loop that effectively traps **TCN** within the active site.<sup>57</sup> More importantly, ordering of this loop occurs both with a C16 fatty acid substrate as well as with the current front-line drug **INH** (**Figure 5**).<sup>58,60</sup> However, as previously mentioned, all of the alkyl diaryl ethers do not display this ordering of the active site loop and potentially as a direct result, these compounds do not exhibit slow-onset inhibition.

### III. 2. 1. *Francisella tularensis* Activity.

Interestingly, all of the unsubstituted alkyl diaryl ethers that are shown in **Table 2** are potent slow, tight-binding inhibitors of the ENR within the FASII

pathway from another bacterium, *Francisella tularensis* with residence times upwards of 90 minutes. More importantly, these compounds display excellent *in vivo* efficacy in a mouse model of *F. tularensis* infection.<sup>61</sup> Therefore, it can be hypothesized that for a compound to show efficacy in a MTB model of infection, it must produce this active site loop ordering and optimistically as a result of this, obtain long residence times comparable to **INH** bound to InhA and those seen with the alkyl diaryl ethers in the *F. tularensis* cases.

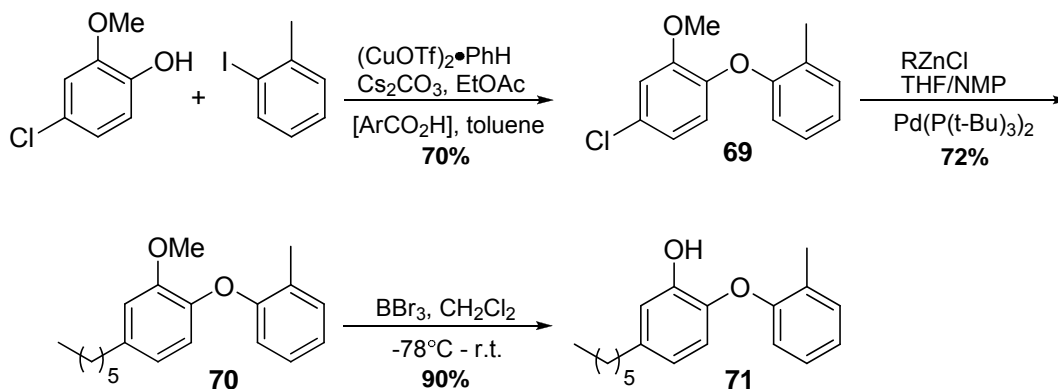
### III. 3. Designing Slow-Onset Inhibitors

Although the concept of slow-onset inhibition might be easy to understand, the ability to engineer this property into a molecular interaction is not surprisingly more difficult. However, since other examples are documented in similar systems, these are a good starting point for analysis. For example, when comparing the structure of the *E. coli* FabI bound to **TCN** where loop ordering is present, with the MTB InhA bound to **5PP**, which does not contain loop ordering, it is evident that **TCN**'s B-ring is almost completely orthogonal with respect to the A-ring whereas this is not the case with **5PP** (**Figure 6a**).<sup>57,59</sup> This may be a result of the *ortho* chlorine residue preferring this orientation pointing down towards the NAD<sup>+</sup>. Furthermore, another consideration is the rotation around the B-ring ether bond. This 'floppiness' of the ring may result in steric impedance to active site loop ordering and may possess an increased entropic penalty of binding compared to **TCN**. The *ortho* chlorine residue on **TCN** may also play a

role in decreasing this rotation. Therefore, in an effort to mimic these effects in conjunction with the knowledge that small substituents are tolerated at the *ortho* position on the B-ring (as shown in the previous chapter **table 4**), compound **71** was synthesized (**scheme 7**).

### III. 4. Chemistry

Compound **71** was synthesized in a manner similar to that used for the previous compounds (**scheme 7**). 4-Chloro-2-methoxyphenol was coupled to iodotoluene under copper-catalyzed Buchwald-Hartwig condition resulting in a reasonable 70% yield, with the lower yield attributed to the increase in steric bulk at the iodine.<sup>72</sup> Next, palladium-catalyzed Negishi coupling of the diaryl ether with hexyl zinc chloride installed the alkyl chain at the 5 position giving compound **70** in 72% yield.<sup>76</sup> Finally, boron tribromide cleavage of the methyl protecting group yielded compound **71** in 90% yield.<sup>74</sup>



**Scheme 7.** Synthesis of the methyl substituted hexyl diaryl ether, **71**.

### III. 5. Results and Discussion

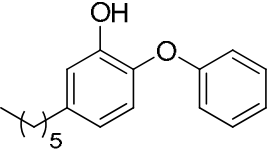
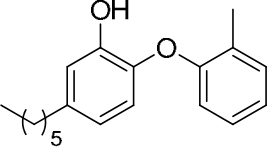
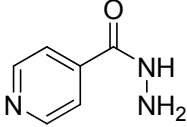
Now, having installed the *ortho* substituent that is similar in size to the *ortho* chlorine on **TCN**, the next step was to determine whether it displayed the desired slow-onset inhibition. Initially, with no preincubation, the  $K_i$  was found to be 560 pM (**Table 6**). Therefore, this was already a marked improvement over the parent compound **6PP**. When a progress curve analysis was performed it was seen that the curve deviated from the standard linear progression thereby demonstrating that inhibition increases over time, consistent with slow-onset inhibition. In order to confirm this, **71** was preincubated with the enzyme for 5 hours which allowed a  $K_i^*$  of  $5.4 \pm 3.1$  pM to be measured (**Table 6**). It was also shown that compound **71** was found to have a dissociative half life of 39 minutes which is comparable to the half life that **INH** displays (**Table 6**).<sup>20</sup> Therefore, these experiments confirmed that there was indeed a slow step that is consistent with the slow-binding mechanism (**Scheme 6b**).

In addition to the kinetic experiments confirming the slow onset type of inhibition consistent with active site loop ordering, a crystal structure was obtained (by Sylvia Luchner at University of Würzburg). **Figure 7a** and **b** shows that unlike with prior alkyl diaryl ether inhibitors which displayed no electron density in this region, **71** displays a clear alpha helix at this locale.<sup>59</sup> Moreover, **71** possesses the desired orthogonal orientation that was seen when **TCN** is bound to FabI (**Figure 6b**).<sup>57</sup> Therefore, the predicted and much to be desired goal of active site loop ordering was achieved. Additional information can be



obtained from this structure as it can be seen that there are further conformational changes within the enzyme. For example, at the backside of the enzyme there is a shift in the helix adjacent to the substrate binding loop that reveals a solvent exposed region at the alkyl chain of the inhibitor (**Figure 7c and d**).<sup>59</sup> This opening may be valuable in the design of further generations of inhibitors that display active site loop ordering.

**Table 6.** **6PP**, **71** and **INH**'s  $K_i$ ,  $K_i^*$ ,  $MIC_{99}$ ,  $ClogP$  and dissociative  $t_{1/2}$  data.

Compound	Structure	$K_i$ (nM) <sup>a</sup>	$K_i^*$ (nM) <sup>b</sup>	$MIC_{99}$ μg/mL (μM) H37 <sub>Rv</sub> <sup>c</sup>	$ClogP^d$	$t_{1/2}$ (min) <sup>e</sup>
<b>6PP</b>		$9.4 \pm 0.5$	N/A	$2.1 \pm 0.9$ ( $7.8 \pm 3.3$ )	6.47	N/A
<b>71</b>		0.560	$0.0054 \pm 0.0031$	0.5 (1.75)	6.97	39
<b>INH</b>		$16 \pm 11^f$	$0.75 \pm 0.08^f$	$0.05 \pm 0$ ( $0.37 \pm 0$ )	-0.67	41

**Table 6** contains the  $MIC_{99}$  inhibition data for compound **71**. It can be seen that the  $MIC_{99}$  value decreases 4-fold with respect to **6PP** with a value of 0.5 μg/mL (1.75 μM) against the H37<sub>Rv</sub> strain of MTB. However, this inhibitor is still 10-fold higher than the  $MIC_{99}$  that is displayed by the current front-line drug **INH**. Furthermore, the  $ClogP$  of this inhibitor has increased to 6.97 from 6.47 for **6PP** thus opposite to the desired values discussed in the previous chapter (**Table 6**).<sup>61</sup> The improved  $MIC_{99}$  value and more importantly the obtaining of the long

residence time within InhA led to compound **71** to be tested in a mouse model of MTB infection. IFN- $\gamma$  GKO mice were infected with MTB and **71** was administered via IP and oral dosing. Despite having all the necessary components for effective *in vivo* activity, this compound displayed no reduction in colony forming units (CFUs).

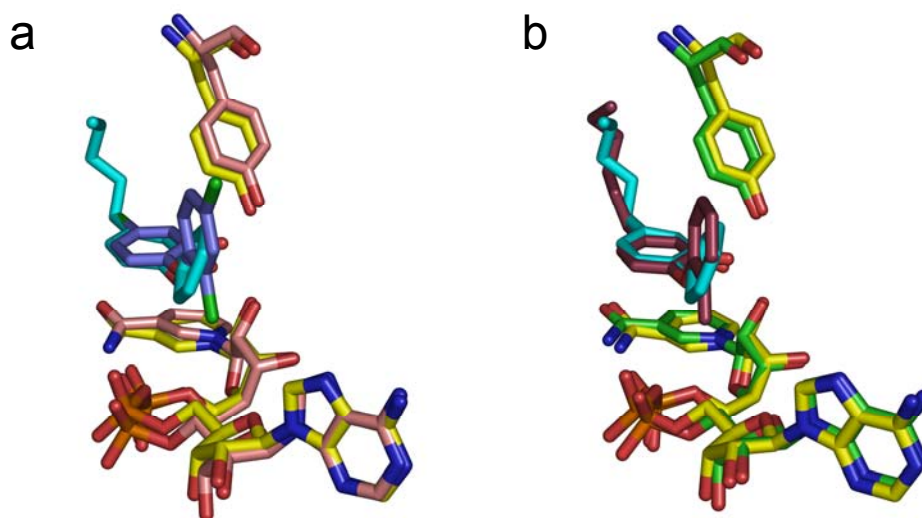


**Figure 6.** Overlay of crystal structures of **a)** triclosan bound to FabI and **5PP** bound to InhA. **b)** **5PP** bound to InhA and compound **71** bound to InhA. Note the similarities in orientation of **71** to that of **TCN**.

Further analysis shows that there is a rapid clearance of the compound from the serum consistent with a metabolic event. Preliminary results reveal that direct glucuronidation of the phenol may be the prevalent route of clearance of this inhibitor and that this process is more prevalent than that with **6PP**. Lastly,

the mode of metabolism of **71** compared with **6PP** needs to be addressed in order to determine how the  $C_{\max}$  and  $t_{1/2}$  can be increased.<sup>61</sup>

### III. 6. Conclusion

In conclusion, a slow, tight-binding inhibitor of the InhA has been synthesized using structure-activity relationship data and crystal structure analysis. It possesses excellent inhibitory properties with a  $K_i^*$  of only 5.4 pM which is more than a 1500-fold improvement above the parent compound **6PP**. In addition, **71** has an  $MIC_{99}$  that is a 4-fold improvement over **6PP**. Despite these excellent inhibitory properties, **71** performed poorly in an *in vivo* environment. Therefore, future efforts will be performed to increase the metabolic stability while retaining its inhibitory properties.

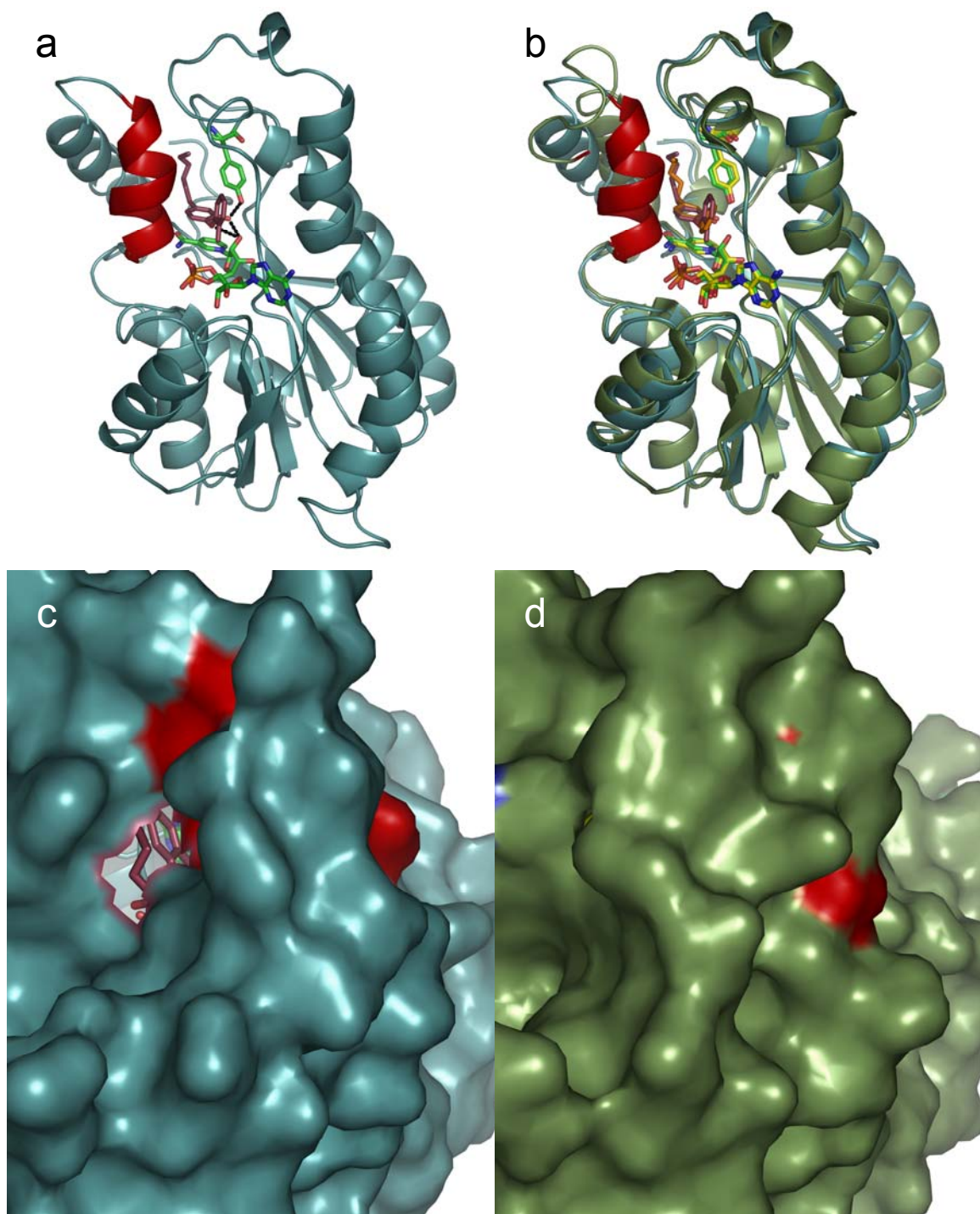


**Figure 7.** Crystal structures of **a)** compound **71** bound to InhA with the ordered loop shown in red. **b)** Overlay of **71** with **5PP**, note the presence of the loop in the **71** structure. **c)** A rear view of the **71** structure showing the solvent accessible aperture that is formed upon loop ordering. **d)** A rear view of the **5PP** crystal structure showing the absence of the solvent accessible hole.

## Chapter IV: Experimental

### IV. 1. General procedures for compound synthesis

**Method A.** The aryl halide (7.35 mmol), phenol (14.7 mmol),  $\text{Cs}_2\text{CO}_3$  (32.3 mmol),  $(\text{CuOTf})_2\cdot\text{PhH}$  (0.735 mmol, 5.0 mol % Cu), ethyl acetate (0.125 mmol, 5.0 mol %), 1-naphthoic acid (32.3 mmol), molecular sieves 4 Å (1.8 g) and toluene (15 mL) were added to a oven-dried 50 mL two-necked round-bottomed flask sealed with a septum which was purged with nitrogen, and heated to 110 °C under nitrogen until completion as determined by TLC. Upon cooling to RT, dichloromethane was added and the organic phase was obtained by filtration. This solution was washed with 5% NaOH. The aqueous layer was then extracted with dichloromethane and the combined organic layers were washed with brine, dried over  $\text{MgSO}_4$  and concentrated under vacuum to give the crude product. The product was then purified by flash chromatography on silica gel (ethyl acetate/hexane).

**Method B.** The aryl halide (50 mmol), 4-bromo-2-methoxyphenol (50 mmol),  $\text{K}_2\text{CO}_3$  (50 mmol) and dimethylacetamide were added to a round-bottomed flask and refluxed for 3h. The resulting mixture was extracted with diethyl ether and washed with 5% KOH and brine. The organic layer was dried over  $\text{MgSO}_4$  and concentrated under vacuum to give the crude product. The product was then purified via crystallization from MeOH or by flash chromatography on silica gel (ethyl acetate/hexane).

**Method C.** ZnCl<sub>2</sub> (0.5 M solution in tetrahydrofuran; 9.0 mL, 4.52 mmol) was added by syringe to a round-bottomed flask sealed with a rubber septum and purged with nitrogen. The appropriate alkyl magnesium chloride (1.0 M solution in THF; 4.0 mL, 4.26 mmol) was then added dropwise by syringe, and the resulting solution was stirred at room temperature for 20 min. *N*-methylpyrrolidinone (4.7 mL) was then added to the flask by syringe, followed by 21.7 mg (0.0426 mmol) of Pd(P(*t*-Bu)<sub>3</sub>)<sub>2</sub> and 500 mg (2.13 mmol) of 4-chloro or bromo-2-methoxy-1-phenoxybenzene after 5 min. The flask was then fitted with a reflux condenser and refluxed for 3-48 h at 130 °C. After cooling gradually to RT, 20 mL of a 1.0 M aqueous HCl solution was added to the flask. The resulting mixture was extracted with diethyl ether, the ether extract was washed with water, and the organic layer was dried over anhydrous MgSO<sub>4</sub> and concentrated under vacuum to give the crude product. The product was purified by flash chromatography on silica gel (ethyl acetate/hexane).

**Method D.** The appropriate nitro compound (2.43 mmol) was added to a solution of EtOH (27 mL) and concentrated HCl (3.8 mL) in a round-bottomed flask. The solution was cooled to 0 °C, and zinc dust (55 mmol) was added in portions over 15 min. The reaction mixture was stirred at RT overnight and the resulting solution was filtered to remove the zinc and reduced *in vacuo*. Diethyl ether was added and the solution was washed with water and brine, dried with

MgSO<sub>4</sub> and concentrated under vacuum to give the crude product. The product was purified via flash chromatography (ethyl acetate/hexane).

**Method E.** The appropriate aniline (1.67 mmol) and triethylamine (2.1 mmol) were added to anhydrous dichloromethane (7 mL) in a nitrogen-flushed round-bottomed flask. The acid chloride (2.1 mmol) was then added dropwise as a solution in anhydrous dichloromethane (1mL) over 25 minutes. After stirring at RT for 3h, the resulting solution was washed successively with 5% HCl, sat. NaHCO<sub>3</sub> and brine. The organic layer was dried over MgSO<sub>4</sub> and reduced under vacuum to give crude product which was then purified by flash chromatography on silica gel (ethyl acetate/hexane).

**Method F.** The benzaldehyde (3.25 mmol) and 1-methyl piperazine (3.25 mmol) were dissolved in dichloroethane (11.5 mL) in a nitrogen-flushed round bottom flask. After 5 minutes, sodium triacetoxyborohydride (4.56 mmol) was added and the solution was stirred at RT for 3h. The reaction was quenched with sat. NaHCO<sub>3</sub>, and extracted with diethyl ether. The organic layer was washed with 5% KOH and brine, dried with MgSO<sub>4</sub> and reduced under vacuum to give the crude product. The product was then purified by flash chromatography (methanol/dichloromethane/ triethylamine).

**Method G.** A solution of boron tribromide in dichloromethane (4 mmol, 1 M solution) was added to a solution of the 4-substituted-2-methoxy-1-phenoxy-

benzene (1.0 mmol) in 5 mL of anhydrous dichloromethane at -78 °C under nitrogen. The reaction mixture was stirred at -78 °C for 1.5 h and then at RT for 3 h. At which point, TLC analysis showed that the reaction had reached completion, the reaction was quenched with methanol at -78 °C and concentrated to give an oil. A suspension of this oil in dichloromethane was washed with 10 % aqueous sodium bicarbonate solution and the organic layer was separated, washed sequentially with water then brine and dried over MgSO<sub>4</sub>. The organic layer was filtered, concentrated under vacuum to give the crude product which was then purified by flash chromatography on silica gel (ethyl acetate/hexane).

#### IV. 2. Compound Characterization

**2-(4-bromo-2-methoxyphenoxy)pyridine (10):** Method B was used to convert 4-bromo-2-methoxy phenol and 2-fluoropyridine to the title product. Purification by flash chromatography (10% EtOAc/Hex) yielded 53% colorless crystals. <sup>1</sup>H NMR (300 MHz, CDCl<sub>3</sub>): δ 3.73 (s, 3H), 6.92-6.98 (m, 2H), 7.01 (dd, *J* = 1.5, 6.0 Hz, 1H), 7.09-7.12 (m, 2H), 7.63-7.69 (m, 1H), 8.11-8.13 (m, 1H).

**3-(4-chloro-2-methoxyphenoxy)pyridine (11):** Method A was used to convert 4-chloro-2-methoxyphenol and 3-iodopyridine to the title product. Purification by flash chromatography (40% EtOAc/Hex) yielded 43% amber oil. <sup>1</sup>H NMR (300



MHz, CDCl<sub>3</sub>):  $\delta$  3.76 (s, 3H), 6.90-6.97 (m, 3H), 7.13-7.20 (m, 2H), 8.26-8.29 (m, 2H); ESI-MS: 236.0 (M+1).

**4-(4-bromo-2-methoxyphenoxy)pyridine (12):** Method B was used to convert 4-bromo-2-methoxyphenol and 4-bromopyridine to the title product. Purification by flash chromatography (15% EtOAc/Hex) yielded 50% amber oil. Compound not characterized.

**2-(4-bromo-2-methoxyphenoxy)pyrazine (13):** Method B was used to convert 4-bromo-2-methoxyphenol and chloropyrazine to the title product. Yield = 97% white powder with no purification needed. <sup>1</sup>H NMR (300 MHz, CDCl<sub>3</sub>):  $\delta$  3.73 (s, 3H), 7.01-7.04 (m, 1H), 7.13 (sextet, *J* = 2.1 Hz, 2H), 8.03 (q, *J* = 1.5 Hz, 1H), 8.23 (d, *J* = 2.4 Hz, 1H), 8.44 (d, *J* = 1.5 Hz, 1H).

**2-(4-bromo-2-methoxyphenoxy)pyrimidine (14):** Method B was used to convert 4-bromo-2-methoxyphenol and chloropyrimidine to the title product. Yield = 55% white powder with no purification needed. <sup>1</sup>H NMR (300 MHz, CDCl<sub>3</sub>):  $\delta$  3.71 (s, 3H), 6.98-7.13 (m, 4H), 8.51 (d, *J* = 4.8 Hz).

**2-(4-bromo-2-methoxyphenoxy)-4,6-dimethoxypyrimidine (15):** Method B was used to convert 4-bromo-2-methoxyphenol and 4,6-dimethoxychloropyrimidine to the title product. Purification by flash chromatography (5% EtOAc/Hex) yielded 42% amber oil. <sup>1</sup>H NMR (300 MHz,

CDCl<sub>3</sub>): δ 3.74 (s, 3H), 3.78 (s, 3H), 3.80 (s, 3H), 6.67 (d, *J* = 8.7 Hz, 1H), 6.91 (d, *J* = 2.7 Hz, 1H), 6.96 (dd, *J* = 2.1, 6.3 Hz, 1H), 6.99-7.04 (m, 1H).

**2-(4-hexyl-2-methoxyphenoxy)pyridine (16):** Method C was used to convert 2-(4-bromo-2-methoxyphenoxy)pyridine to the title product. Purification by flash chromatography (10% EtOAc/Hex) yielded 95% colorless oil. <sup>1</sup>H NMR (300 MHz, CDCl<sub>3</sub>): δ 0.83-0.89 (m, 3H), 1.26-1.36 (m, 6H), 2.58 (t, *J* = 7.5 Hz, 2H), 3.71 (s, 3H), 6.75-6.90 (m, 4H), 6.99 (d, *J* = 8.1 Hz, 1H), 7.55-7.61 (m, 1H), 8.10 (dd, *J* = 1.5, 7.5 Hz, 1H).

**3-(4-hexyl-2-methoxyphenoxy)pyridine (17):** Method C was used to convert 3-(4-chloro-2-methoxyphenoxy)pyridine to the title compound. Purification by flash chromatography (15% EtOAc/Hex) yielded 50% light yellow oil. <sup>1</sup>H NMR (300 MHz, CDCl<sub>3</sub>): δ 0.86-0.90 (m, 3H), 1.29-1.37 (m, 6H), 1.56-1.67 (m, 2H), 2.60 (t, *J* = 7.5 Hz, 2H), 3.77 (s, 3H), 6.74 (dd, *J* = 1.8, 6.3 Hz, 1H), 6.81 (d, *J* = 1.8 Hz, 1H), 6.92 (d, *J* = 7.8 Hz, 1H), 7.13-7.16 (m, 2H), 8.25 (q, *J* = 1.8 Hz, 1H), 8.31 (d, 2.1 Hz, 1H); ESI-MS: 286.1 (M+1).

**4-(4-hexyl-2-methoxyphenoxy)pyridine (18):** Method C was used to convert 4-(4-chloro-2-methoxyphenoxy)pyridine to the title product. Purification by flash chromatography (20% EtOAc/Hex) yielded 89% clear oil. <sup>1</sup>H NMR (300 MHz, CDCl<sub>3</sub>): δ 0.87-0.91 (m, 3H), 1.31-1.36 (m, 6H), 1.59-1.68 (m, 2H), 2.61 (t, *J* =

7.8 Hz, 2H), 3.75 (s, 3H), 6.74-6.83 (m, 4H), 6.97 (d,  $J = 8.1$  Hz, 1H), 8.40 (dd,  $J = 1.5, 3.0$  Hz, 2H); ESI-MS: 286.2 (M+1).

**2-(4-bromo-2-methoxyphenoxy)pyrazine (19):** Method C was used to convert 2-(4-bromo-2-methoxyphenoxy)pyrazine to the title product. Purification by flash chromatography (10% EtOAc/Hex) yielded 77% clear oil.  $^1\text{H}$  NMR (300 MHz,  $\text{CDCl}_3$ ):  $\delta$  0.87-0.92 (m, 3H), 1.25-1.35 (m, 6H), 1.60-1.69 (m, 2H), 2.62 (t,  $J = 8.4$  Hz, 2H), 3.73 (s, 3H), 6.79-6.83 (m, 2H), 7.05 (d,  $J = 7.8$  Hz, 1H), 8.05 (q,  $J = 1.5$  Hz, 1H), 8.20 (d,  $J = 2.7$  Hz, 1H), 8.40 (d,  $J = 1.2$  Hz, 1H).

**2-(4-hexyl-2-methoxyphenoxy)pyrimidine (20):** Method C was used to convert 2-(4-bromo-2-methoxyphenoxy)pyrimidine to the title product. Purification by flash chromatography (10% EtOAc/Hex) yielded 86% clear oil.  $^1\text{H}$  NMR (300 MHz,  $\text{CDCl}_3$ ):  $\delta$  0.86-0.91 (m, 3H), 1.24-1.34 (m, 6H), 1.59-1.68 (m, 2H), 2.60 (t,  $J = 8.1$  Hz, 2H), 3.71 (s, 3H), 6.78-6.81 (m, 2H), 6.96 (t,  $J = 5.1$  Hz, 1H), 7.07 (dd,  $J = 2.4, 7.8$  Hz, 1H), 8.50 (d,  $J = 4.8$  Hz, 2H).

**2-(4-hexyl-2-methoxyphenoxy)-4,6-dimethoxypyrimidine (21):** Method C was used to convert 2-(4-bromo-2-methoxyphenoxy)-4,6-dimethoxypyrimidine to the title product. Purification by flash chromatography (5% EtOAc/Hex) yielded 73% light yellow oil. ESI-MS: 347.1 (M+1).

**5-hexyl-2-(pyridin-2-yloxy)phenol (22):** Method G was used to convert 2-(4-hexyl-2-methoxyphenoxy)pyridine to the title product. Purification by flash chromatography (5% EtOAc/Hex) yielded 76% clear oil. <sup>1</sup>H NMR (300 MHz, CDCl<sub>3</sub>): δ 0.87-0.92 (m, 3H), 1.26-1.39 (m, 6H), 1.52-1.66 (m, 2H), 2.50-2.59 (m, 2H), 6.71 (dd, *J* = 2.1, 7.2 Hz, 1H), 6.92-7.03 (m, 4H), 7.65-7.72 (m, 1H), 8.11 (d, *J* = 4.2 Hz, 1H), 8.20 (bs, 1H); ESI-MS: 272.1 (M+1).

**5-hexyl-2-(pyridin-3-yloxy)phenol (23):** Method G was used to convert 3-(4-hexyl-2-methoxyphenoxy)pyridine to the title product. Purification by flash chromatography (25% EtOAc/Hex) yielded 80% light amber oil. <sup>1</sup>H NMR (300 MHz, CDCl<sub>3</sub>): δ 0.86-0.90 (m, 3H), 1.24-1.38 (m, 6H), 1.54-1.66 (m, 2H), 2.50-2.60 (m, 2H), 6.65-6.76 (m, 1H), 6.86-6.74 (m, 1H), 7.00 (s, 1H), 7.48-7.62 (m, 2H), 8.22-8.48 (m, 3H); ESI-MS: 272.1 (M+1).

**5-hexyl-2-(pyridin-4-yloxy)phenol (24):** Method G was used to convert 4-(4-hexyl-2-methoxyphenoxy)pyridine to the title product. Purification by flash chromatography (20% EtOAc/Hex) yielded 97% clear oil. <sup>1</sup>H NMR (300 MHz, CDCl<sub>3</sub>): δ 0.86-0.88 (m, 3H), 1.22-1.30 (m, 6H), 1.54-1.60 (m, 2), 2.49-2.57 (m, 2H), 6.67-6.93 (m, 5H), 8.22-8.24 (m, 2H); ESI-MS: 272.1 (M+1).

**5-hexyl-2-(pyrazin-2-yloxy)phenol (25):** Method G was used to convert 2-(4-hexyl-2-methoxyphenoxy)pyrazine to the title product. Purification by flash chromatography (15% EtOAc/Hex) yielded 89% white solid. <sup>1</sup>H NMR (300 MHz,

CD<sub>3</sub>OD):  $\delta$  0.87-0.92 (m, 3H), 1.29-1.33 (m, 6H), 1.52-1.64 (m, 2H), 2.49-2.57 (m, 2H), 6.72 (ddd,  $J$  = 1.8, 6.3, 20.7 Hz, 1H), 6.83-6.97 (m, 2H), 8.07-8.08 (m, 1H), 8.19 (q,  $J$  = 1.5 Hz, 1H), 8.31 (d,  $J$  = 0.9 Hz, 1H); ESI-MS: 272.9 (M+1).

**5-hexyl-2-(pyrimidin-2-yloxy)phenol (26):** Method G was used to convert 2-(4-hexyl-2-methoxyphenoxy)pyrimidine to the title product. Purification by flash chromatography (30% EtOAc/Hex) yielded 73% white solid. <sup>1</sup>H NMR (300 MHz, CDCl<sub>3</sub>):  $\delta$  0.84-0.91 (m, 3H), 1.26-1.35 (m, 6H), 1.56-1.63 (m, 2H), 2.52-2.60 (m, 2H), 6.82 (ddd,  $J$  = 2.1, 6.3, 46.5 Hz, 1H), 6.97-7.08 (m, 3H), 7.45 (d,  $J$  = 30.6 Hz, 1H), 8.49 (dd,  $J$  = 1.2, 3.6 Hz, 2H); ESI-MS: 273.4 (M+1).

**2-(4,6-dimethoxypyrimidin-2-yloxy)-5-hexylphenol (27):** Method G was used to convert 2-(4-hexyl-2-methoxyphenoxy)-4,6-dimethoxypyrimidine to the title product. Purification by flash chromatography (10% EtOAc/Hex) yielded 82% light yellow oil. <sup>1</sup>H NMR (300 MHz, CDCl<sub>3</sub>):  $\delta$  0.85-0.91 (m, 3H), 1.27-1.36 (m, 6H), 1.56-1.64 (m, 2H), 2.52-2.59 (m, 2H), 3.86 (s, 6H), 5.80-5.81 (m, 1H), 6.36 (d,  $J$  = 27.9 Hz, 1H), 6.69-7.11 (m, 3H); ESI-MS: 330.0 (M+1).

**4-bromo-2-methoxy-1-(2-nitrophenoxy)benzene (28):** Method B was used to convert 4-bromo-2-methoxyphenol and 2-fluoronitrobenzene to the title product. Recrystallization from methanol yielded 98% light yellow needles. <sup>1</sup>H NMR (300 MHz, CDCl<sub>3</sub>):  $\delta$  3.77 (s, 3H), 6.82 (dd,  $J$  = 1.2, 7.5 Hz, 1H), 6.94 (d,  $J$  = 8.4 Hz,

1H), 7.07-7.16 (m, 3H), 7.41-7.47 (m, 1H), 7.95 (dd,  $J = 1.5, 6.6$  Hz, 1H); ESI-MS: 323.8 (M+1).

**4-bromo-2-methoxy-1-(3-nitrophenoxy)benzene (29):** Method B was used to convert 4-bromo-2-methoxy phenol and 3-fluoronitrobenzene to the title product. Purification by flash chromatography (5% EtOAc/Hex) yielded 65% yellow powder.  $^1\text{H}$  NMR (300 MHz,  $\text{CDCl}_3$ ):  $\delta$  3.79 (s, 3H), 6.97 (d,  $J = 8.4$  Hz, 1H), 7.14 (ddd,  $J = 2.4, 6.0$  Hz, 2H), 7.22-7.26 (m, 1H), 7.45 (t,  $J = 8.1$  Hz, 1H), 7.66 (t,  $J = 2.4$  Hz, 1H), 7.88-7.92 (m, 1H); ESI-MS: 323.7 (M+1).

**4-bromo-2-methoxy-1-(3-nitrophenoxy)benzene (30):** Method B was used to convert 4-bromo-2-methoxy phenol and 4-fluoronitrobenzene to the title product. Recrystallization from methanol yielded 92% light yellow needles.  $^1\text{H}$  NMR (300 MHz,  $\text{CDCl}_3$ ):  $\delta$  3.78 (s, 3H), 6.93 (m, 2H), 6.99 (d,  $J = 8.1$  Hz, 1H), 7.13-7.17 (m, 2H), 8.16-8.19 (m, 2H); ESI-MS: 323.8 (M+1).

**4-bromo-2-methoxy-1-(2-nitrophenoxy)benzene (31):** Method C was used to convert 4-bromo-2-methoxy-1-(2-nitrophenoxy)benzene to the title product. Purification by flash chromatography (5% EtOAc/Hex) yielded 98% yellow crystals.  $^1\text{H}$  NMR (300 MHz,  $\text{CDCl}_3$ ):  $\delta$  0.72-0.78 (m, 3H), 1.12-1.23 (m, 6H), 1.43-1.52 (m, 2H), 2.47 (t,  $J = 7.5$  Hz, 2H), 3.61 (s, 3H), 6.62-6.69 (m, 3H), 6.84 (d,  $J = 8.1$  Hz, 1H), 6.93 (m, 1H), 7.23-7.29 (m, 1H), 7.78 (dd,  $J = 1.8, 6.6$ , 1H); ESI-MS: 330.2 (M+1).

**4-hexyl-2-methoxy-1-(3-nitrophenoxy)benzene (32):** Method C was used to convert 4-bromo-2-methoxy-1-(3-nitrophenoxy)benzene to the title product. Purification by flash chromatography (5% EtOAc/Hex) yielded 95% light yellow oil.  $^1\text{H}$  NMR (300 MHz,  $\text{CDCl}_3$ ):  $\delta$  0.903 (m, 3H), 1.34 (m, 6H), 1.65 (m, 3H), 2.63 (t,  $J = 7.5$  Hz, 2H), 3.78 (s, 3H), 6.78-6.85 (m, 2H), 6.98 (d,  $J = 7.8$  Hz, 1H), 7.22-7.26 (m, 1H), 7.42 (t,  $J = 8.4$  Hz, 1H), 7.66 (t,  $J = 2.1$  Hz, 1H), 7.86 (m, 1H); ESI-MS: 330.0 (M+1).

**4-hexyl-2-methoxy-1-(4-nitrophenoxy)benzene (33):** Method C was used to convert 4-bromo-2-methoxy-1-(4-nitrophenoxy)benzene to the title product. Purification by flash chromatography (5% EtOAc/Hex) yielded 90% light yellow oil.  $^1\text{H}$  NMR (300 MHz,  $\text{CDCl}_3$ ):  $\delta$  0.879-0.923 (m, 3H), 1.13-1.21 (m, 6H), 1.30-1.35 (m, 2H), 2.63 (t,  $J = 7.8$  Hz, 2H), 3.77 (s, 3H), 6.79-6.86 (m, 2H), 6.86-6.87 (m, 2H), 6.99 (d,  $J = 8.1$  Hz, 1H), 8.06-8.09 (m, 2H); ESI-MS: 330.0 (M+1).

**5-hexyl-2-(2-nitrophenoxy)phenol (34):** Method G was used to convert 4-hexyl-2-methoxy-1-(2-nitrophenoxy)benzene to the title product. Purification by flash chromatography (5% EtOAc/Hex) yielded 81% light yellow oil.  $^1\text{H}$  NMR (300 MHz,  $\text{CDCl}_3$ ):  $\delta$  0.87-0.91 (m, 3H), 1.26-1.32 (m, 6H), 1.55-1.64 (m, 2H), 2.57 (t,  $J = 8.1$  Hz, 2H), 6.18 (s, 1H), 6.71 (dd,  $J = 2.1, 6.0$  Hz, 1H), 6.90 (d,  $J = 2.1$  Hz, 1H), 6.96 (d,  $J = 8.1$  Hz, 1H), 7.08 (dd,  $J = 1.5, 6.9$  Hz, 1H), 7.15-7.20 (m, 1H), 7.46-7.51 (m, 1H), 7.90 (dd,  $J = 1.8, 6.3$  Hz, 1H); ESI-MS: 316.0 (M+1).

**5-hexyl-2-(3-nitrophenoxy)phenol (35):** Method G was used to convert 4-hexyl-2-methoxy-1-(3-nitrophenoxy)benzene to the title product. Purification by flash chromatography (5% EtOAc/Hex) yielded 88% light yellow oil. <sup>1</sup>H NMR (300 MHz, CDCl<sub>3</sub>): δ 0.87-0.92 (m, 3H), 1.28-1.38 (m, 6H), 1.57-1.65 (m, 2H), 2.58 (t, *J* = 7.8 Hz, 2H), 5.42 (bs, 1H), 6.72 (dd, *J* = 1.8, 6.3 Hz, 1H), 6.86 (d, *J* = 8.1 Hz, 1H), 6.90 (d, *J* = 2.1 Hz, 1H), 7.30-7.33 (m, 1H), 7.47 (t, *J* = 8.4 Hz, 1H), 7.80 (t, *J* = 2.1 Hz, 1H), 7.92 (tt, *J* = 0.9, 5.1 Hz, 1H); ESI-MS: 316.1 (M+1).

**5-hexyl-2-(4-nitrophenoxy)phenol (36):** Method G was used to convert 4-hexyl-2-methoxy-1-(3-nitrophenoxy)benzene to the title product. Purification by flash chromatography (5% EtOAc/Hex) yielded 92% light yellow oil. <sup>1</sup>H NMR (300 MHz, CDCl<sub>3</sub>): δ 0.87-0.92 (m, 3H), 1.25-1.38 (m, 6H), 1.57-1.65 (m, 2H), 2.56 (t, *J* = 8.1 Hz, 2H), 5.32 (s, 1H), 6.75 (d, *J* = 10.2 Hz, 1H), 6.88-6.91 (m, 2H), 7.02-7.06 (m, 2H), 8.17-8.21 (m, 2H); ESI-MS: 316.3 (M+1).

**2-(4-hexyl-2-methoxyphenoxy)aniline (37):** Method D was used to convert 4-hexyl-2-methoxy-1-(2-nitrophenoxy)benzene to the title product. Purification by flash chromatography (5% EtOAc/Hex) yielded 92% amber oil. <sup>1</sup>H NMR (300 MHz, CDCl<sub>3</sub>): δ 0.91-0.96 (m, 3H), 1.32-1.42 (m, 6H), 1.51-1.52 (m, 2H), 2.62 (t, *J* = 8.1 Hz, 2H), 3.87 (s, 3H), 3.9 (bs, 2H), 6.64-6.73 (m, 2H), 6.57-6.84 (m, 4H), 6.90-6.95 (m, 1H).



**3-(4-hexyl-2-methoxyphenoxy)aniline (38):** Method D was used to convert 4-hexyl-2-methoxy-1-(3-nitrophenoxy)benzene to the title product. Purification by flash chromatography (5% EtOAc/Hex) yielded 98% yellow oil. <sup>1</sup>H NMR (300 MHz, CDCl<sub>3</sub>): δ 0.90-0.94 (m, 3H), 1.29-1.40 (m, 6H), 1.59-1.69 (m, 2H), 2.62 (t, *J* = 9.0 Hz, 2H), 3.64 (bs, 2H), 3.82 (s, 3H), 6.26 (t, *J* = 2.1 Hz, 1H), 6.31-6.36 (m, 2H), 6.74 (dd, *J* = 2.1, 6.0 Hz, 1H), 6.82 (d, *J* = 1.8 Hz, 1H), 6.91 (d, *J* = 8.1 Hz, 1H), 7.04 (t, *J* = 8.4 Hz, 1H); ESI-MS: 300.0 (M+1).

**4-(4-hexyl-2-methoxyphenoxy)aniline (39):** Method D was used to convert 4-hexyl-2-methoxy-1-(4-nitrophenoxy)benzene to the title product. Purification by flash chromatography (5% EtOAc/Hex) yielded 81% reddish oil. <sup>1</sup>H NMR (300 MHz, CDCl<sub>3</sub>): δ 0.89-0.93 (m, 3H), 1.30-1.39 (m, 6H), 1.57-1.66 (m, 2H), 2.58 (t, *J* = 6.0 Hz, 2H), 3.30 (bs, 2H), 3.86 (s, 3H), 6.61-6.64 (m, 2H), 6.67 (dd, *J* = 2.1, 6.3 Hz, 1H), 6.76 (d, *J* = 7.8 Hz, 1H), 6.79-6.84 (m, 4H); ESI-MS: 300.0 (M+1).

**2-(2-aminophenoxy)-5-hexylphenol (40):** Method G was used to convert 2-(4-hexyl-2-methoxyphenoxy)aniline to the title compound. Purification by flash chromatography (10% EtOAc/Hex) yielded 70% light brown solid. <sup>1</sup>H NMR (300 MHz, CDCl<sub>3</sub>): δ 0.87-0.91 (m, 3H), 1.28-1.34 (m, 6H), 1.53-1.63 (m, 2H), 2.54 (t, *J* = 7.8 Hz, 2H), 3.90 (bs, 2H), 6.63 (dd, *J* = 2.1, 6.0 Hz, 1H), 6.71 (td, *J* = 1.2, 6.9 Hz, 1H), 6.78-6.83 (m, 3H), 6.86 (d, *J* = 2.1 Hz, 1H), 6.95 (td, *J* = 1.8, 6.0 Hz, 1H), ESI-MS: 286.1 (M+1).

**2-(3-aminophenoxy)-5-hexylphenol (41):** Method G was used to convert 3-(4-hexyl-2-methoxyphenoxy)aniline to the title compound. Purification by flash chromatography (10% EtOAc/Hex) yielded 75% light brown solid. <sup>1</sup>H NMR (300 MHz, CDCl<sub>3</sub>): δ 0.87-0.92 (m, 3H), 1.26-1.39 (m, 6H), 1.55-1.65 (m, 2H), 2.55 (t, *J* = 8.1 Hz, 2H), 3.73 (bs, 2H), 6.36-6.38 (m, 1H), 6.40 (dt, *J* = 2.4, 3.0 Hz, 2H), 6.70 (dd, *J* = 1.8, 6.6 Hz, 1H), 6.82-6.86 (m, 2H), 7.05 (t, *J* = 8.1 Hz, 1H). ESI-MS: 286.2 (M+1).

**2-(4-aminophenoxy)-5-hexylphenol (42):** Method G was used to convert 4-(4-hexyl-2-methoxyphenoxy)aniline to the title compound. Purification by flash chromatography (10% EtOAc/Hex) yielded 77% light brown solid. <sup>1</sup>H NMR (300 MHz, CDCl<sub>3</sub>): δ 0.86-0.91 (m, 3H), 1.24-1.36 (m, 6H), 1.63-1.63 (m, 2H), 2.53 (t, *J* = 7.8 Hz, 2H), 6.58 (dd, *J* = 1.8, 6.3 Hz, 1H), 6.64-6.69 (m, 3H), 6.83-6.87 (m, 3H); ESI-MS: 286.1 (M+1).

**N-(2-(4-hexyl-2-methoxyphenoxy)phenyl)acetamide (43):** Method E was used to convert 2-(4-hexyl-2-methoxyphenoxy)aniline to the title product. Purification by flash chromatography (5% EtOAc/Hex) yielded 85% white powder. <sup>1</sup>H NMR (300 MHz, CDCl<sub>3</sub>): δ 0.88-0.96 (m, 3H), 1.26-1.38 (m, 6H), 1.59-1.68 (m, 2H), 2.18 (s, 3H), 2.60 (t, *J* = 8.1 Hz, 2H), 3.81 (s, 3H), 6.71-6.76 (m, 2H), 6.81 (d, *J* = 1.8 Hz, 1H), 6.91-7.06 (m, 4H), 8.04 (bs, 1H), 7.41 (d, *J* = 8.1 Hz, 1H).

**N-(3-(4-hexyl-2-methoxyphenoxy)phenyl)acetamide (44):** Method E was used to convert 3-(4-hexyl-2-methoxyphenoxy)aniline to the title product. No purification was necessary. Yielded 98% white powder.  $^1\text{H}$  NMR (300 MHz,  $\text{CDCl}_3$ ):  $\delta$  0.87-0.92 (m, 3H), 1.40-1.48 (m, 6H), 1.57-1.67 (m, 2H), 2.08 (s, 3H), 2.59 (t,  $J = 6.3$  Hz, 2H), 3.79 (s, 3H), 6.62-6.65 (m, 1H), 6.72 (dd,  $J = 2.1, 6.3$ ), 6.80 (d,  $J = 1.8$ , 1H), 6.89 (d,  $J = 7.8$  Hz, 1H), 7.06-7.08 (m, 1H), 7.14-7.23 (m, 2H), 7.55 (bs, 1H); ESI-MS: 342.0 (M+1).

**N-(4-(4-hexyl-2-methoxyphenoxy)phenyl)acetamide (45):** Method E was used to convert 4-(4-hexyl-2-methoxyphenoxy)aniline to the title product. Purification by flash chromatography (5% EtOAc/Hex) yielded 89% white powder.  $^1\text{H}$  NMR (300 MHz,  $\text{CDCl}_3$ ):  $\delta$  0.87-0.93 (m, 3H), 1.30-1.35 (m, 6H), 1.56-1.67 (m, 2H), 2.10 (s, 3H), 2.58 (t,  $J = 7.8$  Hz, 2H), 3.80 (s, 3H), 6.70 (dd,  $J = 2.1, 5.7$  Hz, 1H), 6.79-6.88 (m, 4H), 7.36-7.40 (m, 2H), 7.85 (bs, 1H).

**Methyl-2-(2-(4-hexyl-2-methoxyphenoxy)phenylamino)-2-oxoacetate (46):** Method E was used to convert 3-(4-hexyl-2-methoxyphenoxy)aniline to the title product. No purification was necessary. Yielded 92% light yellow solid. ESI-MS: 386.5 (M+1).

**Methyl-2-(3-(4-hexyl-2-methoxyphenoxy)phenylamino)-2-oxoacetate (47):** Method E was used to convert 3-(4-hexyl-2-methoxyphenoxy)aniline to the title product. No purification was necessary. Yielded 96% light yellow crystals.  $^1\text{H}$

NMR (300 MHz, CDCl<sub>3</sub>):  $\delta$  0.87-0.92 (m, 3H), 1.30-1.37 (m, 6H), 1.58-1.69 (m, 2H), 2.61 (t,  $J$  = 7.5 Hz, 2H), 3.78 (s, 3H), 6.72-6.78 (m, 2H), 6.80 (d,  $J$  = 11.4 Hz, 1H), 6.89-7.07 (m, 2H), 7.16-7.38 (m, 2H), 8.78 (bs, 1H).

**Methyl-2-(4-(4-hexyl-2-methoxyphenoxy)phenylamino)-2-oxoacetate (48):**

Method E was used to convert 4-(4-hexyl-2-methoxyphenoxy)aniline to the title product. No purification was necessary. Yielded 96% light brown solid. <sup>1</sup>H NMR (300 MHz, CDCl<sub>3</sub>):  $\delta$  0.87-0.92 (m, 3H), 1.30-1.40 (m, 6H), 1.59-1.69 (m, 2H), 2.60 (t,  $J$  = 8.1 Hz, 2H), 3.79 (s, 3H), 6.72-6.82 (m, 2H), 6.88-6.96 (m, 3H), 7.14-7.17 (m, 1H), 7.53-7.56 (m, 1H), 8.79 (bs, 1H).

**N-(2-(4-hexyl-2-methoxyphenoxy)phenyl)isoxazole-5-carboxamide (49):**

Method E was used to convert 2-(4-hexyl-2-methoxyphenoxy)aniline to the title product. Purification by flash chromatography (10% EtOAc/Hex) yielded 76% colorless oil. <sup>1</sup>H NMR (300 MHz, CDCl<sub>3</sub>):  $\delta$  0.85-0.89 (m, 3H), 1.24-1.36 (m, 6H), 1.58-1.66 (m, 2H), 2.58 (t,  $J$  = 8.1 Hz, 2H), 3.78 (s, 3H), 6.72-6.81 (m, 3H), 6.96-7.05 (m, 4H), 8.33 (d,  $J$  = 1.8 Hz, 1H), 8.45 (dd,  $J$  = 1.8, 6.0 Hz, 1H), 9.21 (bs, 1H).

**N-(3-(4-hexyl-2-methoxyphenoxy)phenyl)isoxazole-5-carboxamide (50):**

Method E was used to convert 3-(4-hexyl-2-methoxyphenoxy)aniline to the title product. Purification by flash chromatography (25% EtOAc/Hex) yielded 90% white solid. <sup>1</sup>H NMR (300 MHz, CDCl<sub>3</sub>):  $\delta$  0.88-0.92 (m, 3H), 1.28-1.34 (m, 6H),

1.59-1.68 (m, 2H), 2.61 (t,  $J = 7.8$  Hz, 2H), 3.81 (s, 3H), 6.75-6.78 (m, 2H), 6.83 (d,  $J = 1.8$  Hz, 1H), 6.84 (d,  $J = 8.1$  Hz, 1H), 7.00 (dd,  $J = 0.3, 1.5$ , 1H), 7.18 (t,  $J = 2.1$  Hz, 1H), 7.25-7.38 (m, 2H), 8.24 (bs, 1H), 8.35 (dd,  $J = 0.6, 1.5$  Hz, 1H).

**N-(4-(4-hexyl-2-methoxyphenoxy)phenyl)isoxazole-5-carboxamide (51):**

Method E was used to convert 4-(4-hexyl-2-methoxyphenoxy)aniline to the title product. Recrystallization from methanol yielded 75% colorless crystals.  $^1\text{H}$  NMR (300 MHz,  $\text{CDCl}_3$ ):  $\delta$  0.87-0.92 (m, 3H), 1.28-1.34 (m, 6H), 1.60-1.66 (m, 2H), 2.61 (t,  $J = 8.4$  Hz, 2H), 3.82 (s, 3H), 6.74 (dd,  $J = 2.4, 6.0$  Hz, 1H), 6.82 (d,  $J = 1.8$  Hz, 1H), 6.90 (d,  $J = 8.1$  Hz, 1H), 6.93-6.97 (m, 2H), 7.01 (d,  $J = 1.8$  Hz, 1H), 8.19 (bs, 1H), 8.38 (d,  $J = 1.8$  Hz, 1H).

**N-(2-(4-hexyl-2-hydroxyphenoxy)phenyl)acetamide (52):** Method G was used to convert N-(2-(4-hexyl-2-methoxyphenoxy)phenyl)acetamide to the title product. Purification by flash chromatography (10% EtOAc/Hex) yielded 78% white powder.  $^1\text{H}$  NMR (300 MHz,  $\text{CDCl}_3$ ):  $\delta$  0.87-0.92 (m, 3H), 1.29-1.34 (m, 6H), 1.57-1.63 (m, 2H), 2.02 (s, 3H), 2.57 (t,  $J = 7.8$  Hz, 2H), 6.66-6.73 (m, 2H), 6.86-6.90 (m, 2H), 6.99-7.04 (m, 2H), 7.67 (bs, 2H), 7.95-7.83 (m, 1H); ESI-MS: 328.0 (M+1).

**N-(3-(4-hexyl-2-hydroxyphenoxy)phenyl)acetamide (53):** Compound not soluble in a variety of solvents therefore not characterized.

**N-(4-(4-hexyl-2-hydroxyphenoxy)phenyl)acetamide (54):** Method G was used to convert N-(4-(4-hexyl-2-methoxyphenoxy)phenyl)acetamide to the title product. Purification by flash chromatography (12% EtOAc/Hex) yielded 84% white powder. <sup>1</sup>H NMR (300 MHz, CDCl<sub>3</sub>): δ 0.85-0.91 (m, 3H), 1.26-1.36 (m, 6H), 1.54-1.64 (m, 2H), 2.14 (s, 3H), 2.54 (t, *J* = 8.1 Hz, 2H), 5.56 (bs, 1H), 6.63 (dd, *J* = 1.8, 6.3 Hz, 1H), 6.75 (d, *J* = 8.4 Hz, 1H), 6.86 (d, *J* = 2.1 Hz, 1H), 6.89-6.94 (m, 2H), 7.37-7.42 (m, 2H), 7.48 (bs, 1H); ESI-MS: 328.0 (M+1).

**2-(2-(4-hexyl-2-hydroxyphenoxy)phenylamino)-2-oxoacetic acid (55):** Method G was used to convert Methyl-2-(2-(4-hexyl-2-methoxyphenoxy)phenylamino)-2-oxoacetate to the title product. Recrystallization from EtOAc/Hex yielded 70% white crystals. <sup>1</sup>H NMR (300 MHz, Acetone-*d*<sub>6</sub>): δ 0.94-0.99 (m, 3H), 1.36-1.45 (m, 6H), 1.65-1.73 (m, 2H), 2.65 (t, *J* = 6.0 Hz, 2H), 6.76-6.84 (m, 2H), 6.97 (d, *J* = 2.1 Hz, 1H), 7.07-7.21 (m, 3H), 8.22-8.27 (m, 1H), 8.56 (bs, 1H), 9.98 (bs, 1H); ESI-MS: 358.0 (M+1).

**2-(3-(4-hexyl-2-hydroxyphenoxy)phenylamino)-2-oxoacetic acid (56):** Method G was used to convert Methyl-2-(3-(4-hexyl-2-methoxyphenoxy)phenylamino)-2-oxoacetate to the title product. Recrystallization from EtOAc/Hex yielded 65% off-white crystals. <sup>1</sup>H NMR (300 MHz, DMSO-*d*<sub>6</sub>): δ 0.82-0.89 (m, 3H), 1.22-1.34 (m, 6H), 1.49-1.51 (m, 2H), 1.47-2.51 (m, 2H), 6.65-6.64 (m, 2H), 6.76 (s, 1H), 6.85 (d, *J* = 8.1 Hz, 1H), 7.22 (t, *J* = 8.1 Hz, 1H), 7.39 (t, *J* = 10.5 Hz, 2H), 9.34 (s, 1H), 10.66 (s, 1H); ESI-MS: 358.1 (M+1).

**2-(4-(4-hexyl-2-hydroxyphenoxy)phenylamino)-2-oxoacetic acid (57):**

Method G was used to convert Methyl-2-(4-(4-hexyl-2-methoxyphenoxy)phenylamino)-2-oxoacetate to the title product. Recrystallization from EtOAc/Hex yielded 85% white crystals.  $^1\text{H}$  NMR (300 MHz, Acetone- $d_6$ ):  $\delta$  0.98-0.91 (m, 3H), 1.30-1.35 (m, 6H), 1.56-1.66 (m, 2H), 2.56 (t,  $J = 9.1$  Hz, 2H), 6.70 (dd,  $J = 2.1$ , 6.3 Hz, 1H), 6.86-6.93 (m, 4H), 7.78 (dd,  $J = 1.2$ , 7.8 Hz, 2H), 8.14 (bs, 1H), 9.96 (bs, 1H); ESI-MS: 358.1 (M+1).

**N-(2-(4-hexyl-2-hydroxyphenoxy)phenyl)isoxazole-5-carboxamide (58):**

Method G was used to convert N-(2-(4-hexyl-2-methoxyphenoxy)phenyl)isoxazole-5-carboxamide to the title product. Recrystallization from methanol yielded 92% white crystals.  $^1\text{H}$  NMR (300 MHz,  $\text{CDCl}_3$ ):  $\delta$  0.87-0.92 (m, 3H), 1.28-1.37 (m, 6H), 1.59-1.63 m, 2H), 2.56 (t,  $J = 7.8$  Hz, 2H), 6.71 (dd,  $J = 1.8$ , 6.3 Hz, 1H), 6.76 (d,  $J = 7.8$  Hz, 1H), 6.81-6.92 (m, 3H), 7.00-7.1 (m, 3H), 7.97 (dd,  $J = 1.8$ , 6.3 Hz, 1H), 8.35 (s, 1H), 8.75 (bs, 1H); ESI-MS: 381.1 (M+1).

**N-(3-(4-hexyl-2-hydroxyphenoxy)phenyl)isoxazole-5-carboxamide (59):**

Method G was used to convert N-(3-(4-hexyl-2-methoxyphenoxy)phenyl)isoxazole-5-carboxamide to the title product. Purification by flash chromatography (10% EtOAc/Hex) yielded 95% colorless crystals.  $^1\text{H}$  NMR (300 MHz,  $\text{CDCl}_3$ ):  $\delta$  0.87-0.91 (m, 3H), 1.26-1.36 (m, 6H), 1.58-1.62 (m, 2H), 2.56 (t,  $J = 7.5$  Hz, 2H), 5.12 (bs, 1H), 6.68 (dd,  $J = 1.8$ , 6.3 Hz, 1H), 6.79-6.82 (m, 1H),

6.84-6.89 (m, 2H), 7.01 (d,  $J = 1.8$  Hz, 1H), 7.27-7.32 (m, 1H), 7.35-7.38 (m, 2H), 8.32 (bs, 1H), 8.35 (d,  $J = 1.8$  Hz, 1H); ESI-MS: 381.1 (M+1).

**N-(4-(4-hexyl-2-hydroxyphenoxy)phenyl)isoxazole-5-carboxamide (60):**

Method G was used to convert N-(4-(4-hexyl-2-methoxyphenoxy)phenyl)isoxazole-5-carboxamide. Purification by flash chromatography (25% EtOAc/Hex) yielded 93% white solid.  $^1\text{H}$  NMR (300 MHz,  $\text{CDCl}_3$ ):  $\delta$  0.87-0.91 (m, 3H), 1.25-1.39 (m, 6H), 1.55-1.63 (m, 2H), 2.56 (t,  $J = 7.8$  Hz, 2H), 5.50 (s, 1H), 6.67 (dd,  $J = 2.4, 6.0$  Hz, 1H), 6.80 (d,  $J = 8.1$  Hz, 1H), 6.88 (d,  $J = 2.1$  Hz, 1H), 7.02-7.05 (m, 3H), 7.58-7.62 (m, 2H), 8.22 (bs, 1H), 8.39 (d,  $J = 1.2$  Hz, 1H); ESI-MS: 381.1 (M+1).

**2-(4-bromo-2-methoxyphenoxy)benzaldehyde (61):** Method B was used to convert 4-bromo-2-methoxyphenol and 2-fluorobenzaldehyde to give the title product. Purification by flash chromatography (5% EtOAc/Hex) yielded 95% colorless crystals.  $^1\text{H}$  NMR (300 MHz,  $\text{CDCl}_3$ ):  $\delta$  3.76 (s, 3H), 6.68 (dd,  $J = 0.9, 7.5$  Hz, 1H), 6.92 (d,  $J = 8.7$  Hz, 1H), 7.06-7.13 (m, 3H), 7.40-7.46 (m, 1H), 7.88 (dd,  $J = 1.8, 5.7$  Hz, 1H), 10.57 (s, 1H).

**4-(4-bromo-2-methoxyphenoxy)benzaldehyde (62):** Method B was used to convert 4-bromo-2-methoxyphenol and 4-fluorobenzaldehyde to give the title product. Purification by flash chromatography (5% EtOAc/Hex) yielded 97% colorless crystals.  $^1\text{H}$  NMR (300 MHz,  $\text{CDCl}_3$ ):  $\delta$  3.88 (s, 3H), 7.04-7.09 (m, 3H),



7.23 (dd,  $J = 2.1, 6.3$  Hz, 1H), 7.26 (d,  $J = 1.8$  Hz, 1H), 7.90-7.94 (m, 2H), 10.01 (s, 1H).

**1-(2-(4-bromo-2-methoxyphenoxy)benzyl)-4-methylpiperazine (63):** Method F was used to convert 2-(4-bromo-2-methoxyphenoxy)benzaldehyde to the title product. No Purification was necessary. Yielded 86% light brown solid.  $^1\text{H}$  NMR (300 MHz,  $\text{CDCl}_3$ ):  $\delta$  2.24 (s, 3H), 2.38 (bs, 4H), 2.50 (bs, 4H), 3.58 (s, 2H), 3.81 (s, 2H), 6.62 (d,  $J = 8.7$  Hz, 1H), 6.73 (dd,  $J = 1.5, 6.6$  Hz, 1H), 6.95 (dd,  $J = 2.1, 6.3$  Hz, 1H), 7.03-7.08 (m, 2H), 7.14 (td,  $J = 1.8, 6.0$  Hz, 1H), 7.44 (dd,  $J = 1.5, 5.7$  Hz, 1H); ESI-MS: 391.0 (M+1).

**1-(4-(4-bromo-2-methoxyphenoxy)benzyl)-4-methylpiperazine (64):** Method F was used to convert 4-(4-bromo-2-methoxyphenoxy)benzaldehyde to the title product. No Purification was necessary. Yielded 98% off-white crystals.  $^1\text{H}$  NMR (300 MHz,  $\text{CDCl}_3$ ):  $\delta$  2.24 (s, 3H), 2.41 (bs, 8H), 3.42 (s, 2H), 3.78 (s, 3H), 6.77 (d,  $J = 8.7$  Hz, 1H), 6.81-6.85 (m, 2H), 6.98 (dd,  $J = 2.4, 6.3$  Hz, 1H), 7.06 (d,  $J = 2.4$  Hz, 1H), 7.17-7.21 (m, 2H); ESI-MS: 391.0 (M+1).

**1-(2-(4-hexyl-2-methoxyphenoxy)benzyl)-4-methylpiperazine (65):** Method C was used to convert 1-(2-(4-bromo-2-methoxyphenoxy)benzyl)-4-methylpiperazine to the title product. No purification necessary 50% light brown oil. Compound was not characterized.

**1-(4-(4-hexyl-2-methoxyphenoxy)benzyl)-4-methylpiperazine (66):** Method C was used to convert 1-(4-(4-bromo-2-methoxyphenoxy)benzyl)-4-methylpiperazine to the title product. No purification necessary. Yielded 65% light brown oil.  $^1\text{H NMR}$  (300 MHz,  $\text{CDCl}_3$ ):  $\delta$  0.81-0.86 (m, 3H), 1.23-1.30 (m, 6H), 1.51-1.62 (m, 2H), 2.20 (s, 3H), 2.38 (bs, 8H), 2.53 (t,  $J = 6.3$  Hz, 2H), 3.88 (s, 3H), 3.72 (s, 3H), 6.64 (dd,  $J = 2.1, 6.0$  Hz, 1H), 6.74 (d,  $J = 1.8$  Hz, 1H), 6.80 (m, 3H), 7.14 (m, 2H).

**5-hexyl-2-(2-((4-methylpiperazin-1-yl)methyl)phenoxy)phenol (67):** Method G was used to convert 1-(2-(4-hexyl-2-methoxyphenoxy)benzyl)-4-methylpiperazine to the title product. Recrystallized from EtOAc/Hex to yield 72% white crystals.  $^1\text{H NMR}$  (300 MHz,  $\text{CDCl}_3$ ):  $\delta$  0.86-0.91 (m, 3H), 1.26-1.31 (m, 6H), 1.55-1.62 (m, 2H), 2.54 (t,  $J = 7.8$  Hz, 2H), 2.70-2.78 (m, 2H), 3.07 (d,  $J = 13.2$  Hz, 2H), 3.19 (s, 3H), 3.46 (d,  $J = 13.5$  Hz, 2H), 3.82 (s, 2H), 4.15-4.24 (m, 2H), 6.68 (dd,  $J = 1.8, 6.3$  Hz, 1H), 6.77 (d,  $J = 1.8$  Hz, 1H), 6.98 (q,  $J = 8.1$  Hz, 2H), 7.20 (m, 3H), 9.45 (bs, 1H); ESI-MS: 383.3 (M+1).

**5-hexyl-2-(4-((4-methylpiperazin-1-yl)methyl)phenoxy)phenol (68):** Method G was used to convert 1-(4-(4-hexyl-2-methoxyphenoxy)benzyl)-4-methylpiperazine to the title product. Recrystallization from EtOAc/Hex yielded 84% white crystals.  $^1\text{H NMR}$  (300 MHz,  $\text{DMSO}-d_6$ ):  $\delta$  0.83-0.87 (m, 3H), 1.25-1.28 (m, 6H), 1.48-1.58 (m, 2H), 2.46-2.48 (m, 2H), 2.51-2.62 (m, 2H), 2.75-2.86 (m, 2H), 3.02 (s, 3H), 3.35-3.38 (m, 2H), 3.48-3.52 (m, 2H), 3.65-3.76 (m, 2H),

6.61 (dd,  $J = 1.8, 6.0$  Hz, 1H), 6.76-6.85 (m, 5H), 7.20-7.23 (m, 2H), 9.34 (s, 1H);  
ESI-MS: 383.2 (M+1).

**4-chloro-2-methoxy-1-(o-tolyloxy)benzene (69):** Method A was used to convert 4-chloro-2-methoxyphenol and iodotoluene to the title product. Purification by flash chromatography (5% EtOAc/Hex) yielded 70% colorless oil.  $^1\text{H}$  NMR (300 MHz,  $\text{CDCl}_3$ ):  $\delta$  2.31 (s, 3H), 3.88 (s, 3H), 6.69 (d,  $J = 8.7$  Hz, 1H), 6.78 (dd,  $J = 1.2, 6.9$  Hz, 1H), 6.86 (dd,  $J = 2.4$  Hz, 6.3, 1H), 6.99 (d,  $J = 2.4$  Hz, 1H), 7.02-7.07 (m, 1H), 7.11-7.18 (m, 1H), 7.24-7.27 (m, 1H); ESI-MS: 249.1 (M+1)

**4-hexyl-2-methoxy-1-(o-tolyloxy)benzene (70):** Method C was used to convert 4-chloro-2-methoxy-1-(o-tolyloxy)benzene to the title product. Purification by flash chromatography (5% EtOAc/Hex) yielded 72% slightly yellow oil.  $^1\text{H}$  NMR (300 MHz,  $\text{CDCl}_3$ ):  $\delta$  0.94-0.97 (m, 3H), 1.36-1.39 (m, 6H), 1.63-1.72 (m, 2H), 2.38 (s, 3H), 2.54 (t,  $J = 6.0$  Hz, 2H), 3.89 (s, 3H), 6.71-6.80 (m, 3H), 6.86 (d,  $J = 1.5$  Hz, 1H), 6.92-7.04 (m, 1H), 7.10-7.16 (m, 1H), 7.24-2.27 (m, 1H); ESI-MS: 299.2 (M+1).

**5-hexyl-2-(o-tolyloxy)phenol (71):** Method G was used to convert 4-hexyl-2-methoxy-1-(o-tolyloxy)benzene to the title product. Purification by flash chromatography (5% EtOAc/Hex) yielded 90% light yellow oil.  $^1\text{H}$  NMR (400 MHz,  $\text{CDCl}_3$ ):  $\delta$  0.89 (t,  $J = 6.4$  Hz, 3H), 1.28-1.35 (m, 6H), 1.54-1.61 (m, 2H),

2.29 (s, 3H), 2.54 (t,  $J = 6.0$  Hz, 2H), 5.53 (s, 1H), 6.60 (s, 2H), 6.84-6.87 (m, 2H), 7.07 (t,  $J = 6.4$  Hz, 1H), 7.12-7.16 (m, 1H), 7.24 (s, 1H); ESI-MS: 285.3 (M+1).

#### **IV. 3. Kinetic Experiments** – performed by Nina Liu and Hua Xu at Stony Brook University

Kinetic assays using *trans*-2-dodecenoyl-Coenzyme A (DD-CoA) and wild-type InhA were performed as described previously.<sup>22</sup> Reactions were initiated by addition of substrate to solutions containing InhA, inhibitor, and NADH in 30 mM PIPES and 150 mM NaCl, pH 6.8 buffer. IC<sub>50</sub> values were determined by varying the concentration of inhibitor in reactions containing 250 μM NADH, 100 nM InhA and 25 μM DD-CoA. The experimental data were analyzed using eq 1, where I is the inhibitor concentration and y is percent activity, using a slope factor (s) of 1.0.

$$y = 100\% / [1 + (I/IC_{50})^s] \quad (1).$$

Data fitting was performed using Grafit 4.0 (Erithacus Software Ltd.).

#### **IV. 4. Antibacterial Activity** – Performed by Melissa Boyne and Susan Knudson at Colorado State University

MIC<sub>90</sub> data were acquired essentially as described previously using the microplate dilution assay.<sup>31, 32</sup> Briefly, bacterial cells were grown to early-mid log

phase in Middlebrook 7H9 liquid medium containing 10% OADC enrichment and 0.05% Tween-80. Fifty  $\mu\text{L}$  of bacteria were added to the test wells and compounds were added to a final volume of 100  $\mu\text{L}$  per well in 2 fold serial dilutions. Each drug dilution series was performed in triplicate. Plates were incubated at 37°C for 5-7 days and each well was evaluated for growth or no growth. The MIC was the lowest drug concentration that inhibited visible bacterial growth in all replicates. Where alamarBlue® was used as the growth indicator, then the MIC was the lowest drug concentration that maintained a blue color in all replicates. A blue color in the alamarBlue® Assay indicates no bacterial growth and a red color in the assay is indicative of cell growth (BioSource International, Inc).

**IV. 5. LogP Determination** – Performed by James Childs and Charles Peloquin at the National Jewish Medical and Research Center.

The log P value is defined as the partitioning coefficient of a compound in a water iso-octane mixture. In order to estimate log P, an HPLC method was used to establish a standard curve using a series of compounds with known log P values. Compounds were chromatographed on a Phenomenex Bondclone 10  $\mu$  C18 150 x 3.9 mm column using 0.05 M ammonium acetate pH 7.4 as buffer A and acetonitrile as buffer B. The initial solvent conditions were 95%A and 5% B, and after injecting the compounds a linear gradient was applied in which the amount

of A was varied from 95% to 10% over 11 min. The flow rate was 1 mL/min and compounds were detected at 280 nm.

The standards used were as follows (log P values are given in parentheses). Benzo(g,h,i)perylene (6.50), benzo(k)fluoranthene (5.8), nelfinavir (5.53), efavirenz (4.69), imipramine (4.42), quinoline (2.30), ethionamide (1.52), benzamide (0.64), pyrazinamide (-0.53), isoniazid (-0.80). The retention time versus the published log P values were plotted to create a calibration curve and the HPLC retention times of the unknowns were then compared to the calibration curve to obtain an approximate log P of the unknown compounds. .

## References

- (1) Pearce-Duvel, J. M. *Biol. Rev. Camb. Philos. Soc.* **2006**, *81*, 369-382.
- (2) Zink, A. R.; Sola, C.; Reischl, U.; Grabner, W.; Rastogi, N.; Wolf, H.; Nerlich, A. G. *J Clin Microbiol* **2003**, *41*, 359-67.
- (3) Dubos, R., Dubos, J. *The White Plague: Tuberculosis, Man, and Society*; Rutgers University Press: New Brunswick, 1952.
- (4) Schatz, A., Bugie, E., Waksman, S. A. *Proc. Soc. Exper. Biol. Med.* **1944**, *55*, 66-69.
- (5) Lehmann, J. *Dis Chest* **1949**, *16*, 684-703, illust.
- (6) Steenken, W., Jr.; Wolinsky, E. *Trans Annu Meet Natl Tuberc Assoc* **1952**, *48*, 425-30.
- (7) Schwartz, W. S.; Moyer, R. E. *Am Rev Tuberc* **1954**, *70*, 413-22.
- (8) Mulinos, M. G. *Antibiot Annu* **1955**, *3*, 131-5.
- (9) Pilheu, J. A.; Cetrangolo, A. *Rev Asoc Med Argent* **1962**, *76*, 513-4.
- (10) Maggi, N.; Pasqualucci, C. R.; Ballotta, R.; Sensi, P. *Chemotherapy* **1966**, *11*, 285-92.
- (11) Organization, W. H. *Fact sheet on tuberculosis*, 2005.
- (12) Brennan, P. J.; Rooney, S. A.; Winder, F. G. *Ir J Med Sci* **1970**, *3*, 269-84.
- (13) Banerjee, A.; Dubnau, E.; Quemard, A.; Balasubramanian, V.; Um, K. S.; Wilson, T.; Collins, D.; de Lisle, G.; Jacobs, W. R., Jr. *Science* **1994**, *263*, 227-30.
- (14) Dessen, A.; Quemard, A.; Blanchard, J. S.; Jacobs, W. R., Jr.; Sacchettini, J. C. *Science* **1995**, *267*, 1638-41.
- (15) Quemard, A.; Sacchettini, J. C.; Dessen, A.; Vilcheze, C.; Bittman, R.; Jacobs, W. R., Jr.; Blanchard, J. S. *Biochemistry* **1995**, *34*, 8235-41.
- (16) Payne, D. J.; Warren, P. V.; Holmes, D. J.; Ji, Y.; Lonsdale, J. T. *Drug Discov Today* **2001**, *6*, 537-544.
- (17) Zhang, Y.; Heym, B.; Allen, B.; Young, D.; Cole, S. *Nature* **1992**, *358*, 591-3.
- (18) Johnsson, K., King, D.S., Schultz, P.G. *J. Am. Chem. Soc.* **1995**, *117*, 5009-5010.
- (19) Marcinkeviciene, J. A. M., R.S., Blanchard, J.S. *J. Biol. Chem.* **1995**, *270*.
- (20) Rawat, R.; Whitty, A.; Tonge, P. J. *Proc Natl Acad Sci U S A* **2003**, *100*, 13881-6.
- (21) Stoeckle, M. Y.; Guan, L.; Riegler, N.; Weitzman, I.; Kreiswirth, B.; Kornblum, J.; Laraque, F.; Riley, L. W. *J Infect Dis* **1993**, *168*, 1063-5.
- (22) Musser, J. M.; Kapur, V.; Williams, D. L.; Kreiswirth, B. N.; van Soolingen, D.; van Embden, J. D. *J Infect Dis* **1996**, *173*, 196-202.
- (23) Ramaswamy, S. V.; Reich, R.; Dou, S. J.; Jasperse, L.; Pan, X.; Wanger, A.; Quitugua, T.; Graviss, E. A. *Antimicrob Agents Chemother* **2003**, *47*, 1241-50.
- (24) Kuo, M. R.; Morbidoni, H. R.; Alland, D.; Sneddon, S. F.; Gourlie, B. B.; Staveski, M. M.; Leonard, M.; Gregory, J. S.; Janjigian, A. D.; Yee, C.;

- Musser, J. M.; Kreiswirth, B.; Iwamoto, H.; Perozzo, R.; Jacobs, W. R., Jr.; Sacchettini, J. C.; Fidock, D. A. *J Biol Chem* **2003**, *278*, 20851-9.
- (25) He, X.; Alian, A.; Stroud, R.; Ortiz de Montellano, P. R. *J Med Chem* **2006**, *49*, 6308-23.
- (26) He, X.; Alian, A.; Ortiz de Montellano, P. R. *Bioorg Med Chem* **2007**, *15*, 6649-58.
- (27) Lu, H.; Tonge, P. J. *Acc Chem Res* **2008**, *41*, 11-20.
- (28) de Boer, G. J.; Pielage, G. J.; Nijkamp, H. J.; Slabas, A. R.; Rafferty, J. B.; Baldock, C.; Rice, D. W.; Stuitje, A. R. *Mol Microbiol* **1999**, *31*, 443-50.
- (29) Levy, C. W.; Roujeinikova, A.; Sedelnikova, S.; Baker, P. J.; Stuitje, A. R.; Slabas, A. R.; Rice, D. W.; Rafferty, J. B. *Nature* **1999**, *398*, 383-4.
- (30) Heath, R. J.; White, S. W.; Rock, C. O. *Appl Microbiol Biotechnol* **2002**, *58*, 695-703.
- (31) Nomura, S.; Horiuchi, T.; Omura, S.; Hata, T. *J Biochem* **1972**, *71*, 783-96.
- (32) Noto, T.; Miyakawa, S.; Oishi, H.; Endo, H.; Okazaki, H. *J Antibiot (Tokyo)* **1982**, *35*, 401-10.
- (33) Tsay, J. T.; Rock, C. O.; Jackowski, S. *J Bacteriol* **1992**, *174*, 508-13.
- (34) Kremer, L.; Douglas, J. D.; Baulard, A. R.; Morehouse, C.; Guy, M. R.; Alland, D.; Dover, L. G.; Lakey, J. H.; Jacobs, W. R., Jr.; Brennan, P. J.; Minnikin, D. E.; Besra, G. S. *J Biol Chem* **2000**, *275*, 16857-64.
- (35) Price, A. C.; Choi, K. H.; Heath, R. J.; Li, Z.; White, S. W.; Rock, C. O. *J Biol Chem* **2001**, *276*, 6551-9.
- (36) Chirala, S. S.; Huang, W. Y.; Jayakumar, A.; Sakai, K.; Wakil, S. J. *Proc Natl Acad Sci U S A* **1997**, *94*, 5588-93.
- (37) Campbell, J. W.; Cronan, J. E., Jr. *Annu Rev Microbiol* **2001**, *55*, 305-32.
- (38) Chung, G. A.; Aktar, Z.; Jackson, S.; Duncan, K. *Antimicrob Agents Chemother* **1995**, *39*, 2235-8.
- (39) Dunn, D.; Orłowski, M.; McCoy, P.; Gastgeb, F.; Appell, K.; Ozgur, L.; Webb, M.; Burbaum, J. *J Biomol Screen* **2000**, *5*, 177-88.
- (40) White, E. L.; Southworth, K.; Ross, L.; Cooley, S.; Gill, R. B.; Sosa, M. I.; Manouvakhova, A.; Rasmussen, L.; Goulding, C.; Eisenberg, D.; Fletcher, T. M., 3rd *J Biomol Screen* **2007**, *12*, 100-5.
- (41) Davies, J. W.; Glick, M.; Jenkins, J. L. *Curr Opin Chem Biol* **2006**, *10*, 343-51.
- (42) Bissantz, C.; Folkers, G.; Rognan, D. *J Med Chem* **2000**, *43*, 4759-67.
- (43) Schneider, G.; Bohm, H. J. *Drug Discov Today* **2002**, *7*, 64-70.
- (44) Amyes, T. L.; Richard, J. P. *ACS Chem Biol* **2007**, *2*, 711-4.
- (45) Schramm, V. L. *J Biol Chem* **2007**, *282*, 28297-300.
- (46) Lewandowicz, A.; Shi, W.; Evans, G. B.; Tyler, P. C.; Furneaux, R. H.; Basso, L. A.; Santos, D. S.; Almo, S. C.; Schramm, V. L. *Biochemistry* **2003**, *42*, 6057-66.
- (47) Freundlich, J. S.; Anderson, J. W.; Sarantakis, D.; Shieh, H. M.; Yu, M.; Valderramos, J. C.; Lucumi, E.; Kuo, M.; Jacobs, W. R., Jr.; Fidock, D. A.; Schiehser, G. A.; Jacobus, D. P.; Sacchettini, J. C. *Bioorg Med Chem Lett* **2005**, *15*, 5247-52.



- (48) Freundlich, J. S.; Yu, M.; Lucumi, E.; Kuo, M.; Tsai, H. C.; Valderramos, J. C.; Karagyoov, L.; Jacobs, W. R., Jr.; Schiehser, G. A.; Fidock, D. A.; Jacobus, D. P.; Sacchettini, J. C. *Bioorg Med Chem Lett* **2006**, *16*, 2163-9.
- (49) Anquetin, G.; Greiner, J.; Mahmoudi, N.; Santillana-Hayat, M.; Gozalbes, R.; Farhati, K.; Derouin, F.; Aubry, A.; Cambau, E.; Vierling, P. *Eur J Med Chem* **2006**, *41*, 1478-93.
- (50) Sivaraman, S.; Sullivan, T. J.; Johnson, F.; Novichenok, P.; Cui, G.; Simmerling, C.; Tonge, P. J. *J Med Chem* **2004**, *47*, 509-18.
- (51) Heath, R. J.; White, S. W.; Rock, C. O. *Prog Lipid Res* **2001**, *40*, 467-97.
- (52) McMurry, L. M.; McDermott, P. F.; Levy, S. B. *Antimicrob Agents Chemother* **1999**, *43*, 711-3.
- (53) Heath, R. J.; Li, J.; Roland, G. E.; Rock, C. O. *J Biol Chem* **2000**, *275*, 4654-9.
- (54) Surolia, N.; Surolia, A. *Nat Med* **2001**, *7*, 167-73.
- (55) Ward, W. H.; Holdgate, G. A.; Rowsell, S.; McLean, E. G.; Pauptit, R. A.; Clayton, E.; Nichols, W. W.; Colls, J. G.; Minshull, C. A.; Jude, D. A.; Mistry, A.; Timms, D.; Camble, R.; Hales, N. J.; Britton, C. J.; Taylor, I. W. *Biochemistry* **1999**, *38*, 12514-25.
- (56) Parikh, S. L.; Xiao, G.; Tonge, P. J. *Biochemistry* **2000**, *39*, 7645-50.
- (57) Stewart, M. J.; Parikh, S.; Xiao, G.; Tonge, P. J.; Kisker, C. *J Mol Biol* **1999**, *290*, 859-65.
- (58) Rozwarski, D. A.; Vilcheze, C.; Sugantino, M.; Bittman, R.; Sacchettini, J. C. *J Biol Chem* **1999**, *274*, 15582-9.
- (59) Sullivan, T. J.; Truglio, J. J.; Boyne, M. E.; Novichenok, P.; Zhang, X.; Stratton, C. F.; Li, H. J.; Kaur, T.; Amin, A.; Johnson, F.; Slayden, R. A.; Kisker, C.; Tonge, P. J. *ACS Chem Biol* **2006**, *1*, 43-53.
- (60) Rozwarski, D. A.; Grant, G. A.; Barton, D. H.; Jacobs, W. R., Jr.; Sacchettini, J. C. *Science* **1998**, *279*, 98-102.
- (61) Results, U.
- (62) Veber, D. F.; Johnson, S. R.; Cheng, H. Y.; Smith, B. R.; Ward, K. W.; Kopple, K. D. *J Med Chem* **2002**, *45*, 2615-23.
- (63) Chaturvedi, P. R.; Decker, C. J.; Odinecs, A. *Curr Opin Chem Biol* **2001**, *5*, 452-63.
- (64) Stoner, C. L.; Cleton, A.; Johnson, K.; Oh, D. M.; Hallak, H.; Brodfuehrer, J.; Surendran, N.; Han, H. K. *Int J Pharm* **2004**, *269*, 241-9.
- (65) Shargel, L., Yu, A.B. *Applied biopharmaceutics & pharmacokinetics*; 4th ed. ed.; McGraw-Hill: New York, 1999.
- (66) Lipinski, C. A.; Lombardo, F.; Dominy, B. W.; Feeney, P. J. *Adv Drug Deliv Rev* **2001**, *46*, 3-26.
- (67) Larsen, T.; Link, A. *Angew Chem Int Ed Engl* **2005**, *44*, 4432-4.
- (68) Bergstrom, C. A.; Strafford, M.; Lazorova, L.; Avdeef, A.; Luthman, K.; Artursson, P. *J Med Chem* **2003**, *46*, 558-70.
- (69) Lu, J. J.; Crimin, K.; Goodwin, J. T.; Crivori, P.; Orrenius, C.; Xing, L.; Tandler, P. J.; Vidmar, T. J.; Amore, B. M.; Wilson, A. G.; Stouten, P. F.; Burton, P. S. *J Med Chem* **2004**, *47*, 6104-7.
- (70) Muegge, I. *Med Res Rev* **2003**, *23*, 302-21.

- (71) Clark, D. E. *J Pharm Sci* **1999**, *88*, 807-14.
- (72) Marcoux, J. F. D., S., Buchwald, S.L. *J. Am. Chem. Soc.* **1997**, *119*, 10539-10540.
- (73) Marsh, G.; Stenutz, R.; Bergman, A. *Eur. J. Org. Chem.* **2003**, 2566-2576.
- (74) Neumeyer, J. L.; Baidur, N.; Yuan, J.; Booth, G.; Seeman, P.; Niznik, H. B. *J Med Chem* **1990**, *33*, 521-6.
- (75) Masesane, I. B.; Batsanov, A. S.; Howard, J. A.; Mondal, R.; Steel, P. G. *Beilstein J. Org. Chem.* **2006**, *2*.
- (76) Dai, C.; Fu, G. C. *J Am Chem Soc* **2001**, *123*, 2719-24.
- (77) Deruiter, J.; Swearingen, B. E.; Wandrekar, V.; Mayfield, C. A. *J. Med. Chem.* **1989**, *32*, 1033-1038.
- (78) Abdel-Magid, A. F.; Carson, K. G.; Harris, B. D.; Maryanoff, C. A.; Shah, R. D. *J. Org. Chem.* **1996**, *61*, 3849-3862.
- (79) Copeland, R. A. *Evaluation of Enzyme Inhibitors in Drug Discovery*, Wiley-Interscience: Hoboken, 2005.
- (80) Copeland, R. A.; Pompliano, D. L.; Meek, T. D. *Nat Rev Drug Discov* **2006**, *5*, 730-9.
- (81) Swinney, D. C. *Nat Rev Drug Discov* **2004**, *3*, 801-8.
- (82) Gooljarsingh, L. T.; Fernandes, C.; Yan, K.; Zhang, H.; Grooms, M.; Johanson, K.; Sinnamon, R. H.; Kirkpatrick, R. B.; Kerrigan, J.; Lewis, T.; Arnone, M.; King, A. J.; Lai, Z.; Copeland, R. A.; Tummino, P. J. *Proc Natl Acad Sci U S A* **2006**, *103*, 7625-30.
- (83) Cayley, P. J.; Albrand, J. P.; Feeney, J.; Roberts, G. C.; Piper, E. A.; Burgen, A. S. *Biochemistry* **1979**, *18*, 3886-95.
- (84) Reynolds, C. H. *Biochem Pharmacol* **1984**, *33*, 1273-6.
- (85) Kati, W. M.; Montgomery, D.; Carrick, R.; Gubareva, L.; Maring, C.; McDaniel, K.; Steffy, K.; Molla, A.; Hayden, F.; Kempf, D.; Kohlbrenner, W. *Antimicrob Agents Chemother* **2002**, *46*, 1014-21.
- (86) Ojima, M.; Inada, Y.; Shibouta, Y.; Wada, T.; Sanada, T.; Kubo, K.; Nishikawa, K. *Eur J Pharmacol* **1997**, *319*, 137-46.
- (87) Chan, C. C.; Boyce, S.; Brideau, C.; Charleson, S.; Cromlish, W.; Ethier, D.; Evans, J.; Ford-Hutchinson, A. W.; Forrest, M. J.; Gauthier, J. Y.; Gordon, R.; Gresser, M.; Guay, J.; Kargman, S.; Kennedy, B.; Leblanc, Y.; Leger, S.; Mancini, J.; O'Neill, G. P.; Ouellet, M.; Patrick, D.; Percival, M. D.; Perrier, H.; Prasit, P.; Rodger, I.; et al. *J Pharmacol Exp Ther* **1999**, *290*, 551-60.